DNA damage associated lncRNAs, PANDA, ANRIL and DDSR1, are constitutively active in HT29 cells under hypertonic stress

By

Aalia Patel

(667992)

Dissertation

Submitted in fulfilment of the Dissertation only degree

MSc

in

Molecular and Cell Biology

in the Faculty of Science, University of the Witwatersrand, Johannesburg, South Africa

Supervisor:

Dr Rupal Jivan

July 2022

Table of Contents

Candidates Declaration ---- **i**

Dedication ---- **ii**

Acknowledgments ---- **iii**

List of Figures ---- **iv**

List of Tables ---- **v**

List of Abbreviations ---- **vi**

Abstract ---- **ix**

1 Introduction ---- ***1***

1.1 Genomic Instability and Cancer ---- **1**

1.2 The MRN Complex ---- **3**

1.2.1 MRN in DSB Sensing ---- 4

1.2.2 H2AX Phosphorylation Signalling ---- 5

1.3 DNA DSBs Repair ---- **5**

1.3.1 Non-Homologous End Joining ---- 6

1.3.2 Homologous Recombination ---- 7

1.4 LncRNAs Regulate DDR and Genomic Stability ---- **8**

1.4.1 LncRNA PANDA ---- 11

1.4.2 LncRNA ANRIL ---- 13

1.4.3 LncRNA DDSR1 ---- 13

1.5 NaCl-Induced DNA Damage ---- **14**

2 Aims and Objectives ---- ***16***

2.1 Aims ---- **16**

2.2 Objectives ---- **16**

3 Methods ---- ***17***

3.1 Lab Reagents ---- **17**

3.2 Cell Culture ---- **17**

3.3 MTT Assay ---- **17**

3.4 Confocal Microscopy ---- 18

3.5 Western Blot ---- 19

3.5.1 Cell Treatment ---- 19

3.5.2 Protein Extraction and Quantification ---- 19

3.5.3 SDS-PAGE and Transfer ---- 20

3.5.4 Antibody Treatments and Detection ---- 21

3.6 RT-PCR and qRT-PCR ---- 21

3.6.1 RNA Extraction ---- 22

3.6.2 cDNA Conversion ---- 22

3.6.3 RT-PCR ---- 23

3.6.4 qRT-PCR ---- 24

3.7 Statistical Analysis ---- 25

4 Results ---- 25

4.1 Higher concentrations of NaCl are required to promote cytotoxicity in HT29 compared to HEK293 cells ---- 25

4.2 Mre11 translocated to the cytoplasm in the presence of NaCl and translocated to the nucleus upon withdrawal in HEK293 and HT29 cells ---- 27

4.3 γH2AX levels are not significantly altered after NaCl treatment in HEK293 and HT29 cell lines ---- 31

4.4 4.4. lncRNA expression in response to NaCl treatment ---- 32

5 Discussion ---- 37

6 Limitations and Future Directions ---- 38

7 Conclusion ---- 39

8 References ---- 40

Candidates Declaration

I, Aalia Patel, (Student number: 667992) am a student at the University of the Witwatersrand, Johannesburg, registered for the degree of Master of Science in Molecular and Cell Biology, in the academic year 2022.

I, hereby declare that the work submitted is my own work. I declare that this work has not been submitted for this degree at this university or any other university.

Signature: 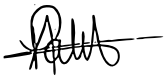 _____ Date: 22 July 2022

Dedication

I dedicate this dissertation to my parents,

Fatima Kotwal and Mohammed Ishad Patel,

for always encouraging me to work hard and accomplish my dreams and for giving me the opportunity to do so.

Acknowledgments

I would like to acknowledge:

My family and friends for supporting me through this journey

Aurelie at Life Science Imaging Facility, for assisting me with obtaining my Confocal Microscopy data

The University of the Witwatersrand for the Postgrad Merit Award

NRF for funding my project

List of Figures

Figure 1: DNA damage response and signalling pathways in response to DNA double-strand breaks. ---------- 2
Figure 2: Biological functions of lncRNAs. ---------- 10
Figure 3: Cell viability assessed by MTT assay. ---------- 26
Figure 4: Mre11 localisation in HEK293 cells assessed by confocal microscopy. -------- 28
Figure 5: Mre11 localisation in HT29 cells assessed by confocal microscopy. ---------- 30
Figure 6: DNA damage repair observed by γH2AX expression by western blot analysis. ---------- 31
Figure 7: LncRNA expression analysis for PANDA, ANRIL and DDSR1 analysed by RT-PCR. ---------- 34
Figure 8: DNA damage associated lncRNA expression of lncRNAs PANDA, ANRIL, and DDSR1 in response to NaCl treatment and withdrawal by qRT-PCR. ---------- 36

List of Tables

Table 1: Polyacrylamide recipe for resolving and stacking gel----------20

Table 2: cDNA synthesis thermocycler run conditions ----------23

Table 3: Forward and reverse Primers for lncRNAs PANDA, ANRIL & DDSR1 and housekeeping gene GAPDH with their respective melting temperatures and annealing temperatures----------23

Table 4: RT-PCR thermocycler conditions----------24

Table 5: Bio-rad CFX96 thermocycler conditions ----------25

Table 6: Statistical significance indicated by asterisks----------25

Table 7: Calculated EC50 and EC30 values determined using DR-Hill equation (CurveExpert Basic) and standard deviations for HEK293 and HT 29 cell lines --------26

List of Abbreviations

53PB1	p53 binding protein
ABC-ATPase	ATP-binding cassette-ATPase
ANRIL	Antisense non-coding RNA in the INK4 locus
APS	Ammonium Persulphste
ARF	p14
ATM	Ataxia Telangiectasia mutated protein
ATR	ATM and Rad3-related kinase
BRCA1	Breast Cancer Susceptibility protein 1
BRCA2	Breast Cancer Susceptibility protein 2
BRCT	Breast Cancer C-terminal
BSA	Bovine Serum Albumin
BSA	Bovine serum albumin
CDK2	Cyclin dependent kinase 2
CDKN1A	Cyclin Dependent Kinase Inhibitor 1A
CDKN2A/B	Cyclin Dependent Kinase Inhibitor 2A/B
CDKs	Cyclin-Dependant Kinases
cDNA	complementary DNA
chk1	Checkpoint Kinase 1
chk2	Checkpoint Kinase 2
CRNDE	Colorectal Neoplasia Differentially Expressed
DAPI	4,6-diamidino-2-phenylindole
DDR	DNA damage response
DDSR1	DNA damage sensitive RNA1
DMEM	Dulbecco's modified eagle medium nutrient mixture
DMSO	Dimethylsulfoxide
DNA-PK	DNA-dependent protein kinase
DNA-PKcs	DNA-dependent protein kinase catalytic subunit
DNMTs	DNA methyltransferases
DNMTs	DNA methyltransferases
DSBs	Double strand breaks
DTT	Dithiothreitol
E2F1	E2F Transcription Factor 1
EDTA	Ethylenediaminetetraacetic acid
FBS	fetal bovine serum
FHA	forkhead associated
ɣH2AX	H2AXSer139ph
hnRNPUL1	heterogenous nuclear ribonucleoprotein U-like protein 1
HOTAIR	HOX antisense intergenic RNA
HOXD	Homeobox D
HR	Homologous recombination
INK4A	p16

INK4B	p15
Ku70 and Ku80	Ku80 Ku70/80 heterodimer
lncRNAs	long non-coding RNAs
MAPK	Mitogen-activated protein kinases
MDC1	Mediator of DNA damage checkpoint protein
Mdm2	Mouse double minute 2 homolog
Mre 11	meiotic recombination 11 homolog 1
MRN	Mre11-Rad50-Nbs1
mRNAs	Messenger RNA
MTT	3-(4,5-dimethylthiazol-2-yl)-2,5-diphenyltetrazolium bromide
NaCl	Sodium Chloride
Nbs1	Nijmegan breakage syndrome protein 1
ncRNA	non-coding RNA
NF-YA	nuclear transcription factor Y subunit alpha
NF-**κ**B	Nuclear factor kappa-B
NFAT5	nuclear factor of activated T cells-5
NHEJ	Non-homologous end joining
NOXA	103 amin acid protein, latin term for damage
ORF	open reading frame
PANDA	p21 associated ncRNA DNA damage activated
PAXX	Paralog of XRCC4 and XLF
PBS	Phosphate-buffered saline
PIKK	Phosphoinositide 3-kinase-related protein kinases
PMSF	phenylmethylsulfonyl fluoride
pol m	DNA Polymersase mu
pol λ	DNA polymerase lambda
pRB	Retinoblastoma protein
PRC	Polycomb Repressive Complex
PRC1 and PRC2	polycomb repressive complexes 1 and 2
PTIP	Pax transactivation domain-interacting protein
PUMA	p53 upregulated modulator of apoptosis
qRT-PCR	quantitaive reverse transcriptase polymerase chain reaction
Rad50	DNA repair protein Rad50
Rap80	receptor-associated protein 80
RBP	RNA-binding proteins
RIF1	Rap1-interacting protein
RIPA	Radioimmunoprecipitation assay
RPA	replication protein A
RT-PCR	Reverse transcriptase Polymersae Chain reaction
SAFA	scaffold-attachment-factor A
SAPK	Stress-activated protien kinase
SDS-PAGE	sodium dodecyl sulfate–polyacrylamide gel electrophoresis

Sp1	Specificty protein 1
SSBs	Single strand breaks
TCA	Trichloroacetic acid
TEMED	Tetramethylethylenediamine
UCA1	Urothelial carcinoma associated 1
WIP1	Wild-type p53-induced Phosphatase 1
XLF	XRCC4-like factor
XRCC4	X-ray cross complementing protein 4

Abstract

Our genomes undergo DNA damage regularly with the most lethal being DNA double-strand breaks (DSBs). Long non-coding RNAs (lncRNAs) have distinct biological functions and play roles in DNA damage response (DDR). We hypothesized that lncRNA expression would be altered in response to NaCl-induced DNA damage and that these effects may be different in cancer and non-cancer cell lines. Exposure of cells to high NaCl concentrations promotes DSBs in DNA regions near the nuclear periphery. These are rapidly repaired after NaCl withdrawal. 3-(4,5-dimethylthiazol-2-yl)-2,5-diphenyl-2H-tetrazolium bromide (MTT) assays were performed on HEK293 and HT29 cell lines to determine the EC50 for NaCl. For confocal microscopy, cells were treated with NaCl for 6 hrs or 24 hrs followed by 5 min NaCl withdrawal, and Mre11 was detected. Results indicated that meiotic recombination 11 homolog 1 (Mre11) was localized in the cytoplasm in the presence of NaCl and translocated to the nucleus during 5 min NaCl withdrawal in HEK293 cells. Under high NaCl, Mre11 was present in both the nucleus and cytoplasm in HT29 cells. DSB assessment by western blot analysis for γH2AX revealed no significant change in expression in HEK293 and HT29 cells, but slightly lower levels in HT29 suggest DNA repair may occur in the presence of NaCl. PCR and qPCR were performed for lncRNAs p21 associated ncRNA DNA damage activated (PANDA), Antisense non-coding RNA in the INK4 locus (ANRIL), and DNA damage sensitive RNA1 (DDSR1). qPCR data shows that PANDA, ANRIL, and DDSR1 expression is reduced in HEK293 during NaCl treatment, while in HT29s PANDA was upregulated in response to NaCl treatment and NaCl withdrawal, ANRIL was only upregulated after 4 hrs NaCl and in the 6 hr 5 min NaCl withdrawal treatment and DDSR1 expression was significantly higher in the 6 hr treatment only. Whilst hyperosmotic stress was used to induce DNA damage, we have observed that it results in reduced expression of lncRNAs that play roles in DNA repair and cell cycle regulation in a non-cancer cell line, and enhanced expression in a cancer cell line. This suggests that in hypertonic environments the HT29 cells may still be undergoing cell cycle arrest, DNA repair, and proliferation.

1 Introduction

1.1 Genomic Instability and Cancer

Cancer is the second highest cause of death worldwide and is mainly characterised by genomic instability, arising from genetic and epigenetic mutations occurring at a more rapid and uncontrolled rate (Hanahan and Weinberg, 2011; Pikor et al., 2013). Genomic instability is the accumulation of large-scale chromosomal aberrations during cell division. Genome stability is maintained through quality DNA replication, accurate and equal chromosome distribution during mitosis, DNA damage response (DDR) pathways that sense DNA strand breaks that occur throughout the cell cycle, and cell cycle checkpoints that regulate cell cycle progression (Shen, 2011). Improper regulation of these mechanisms results in the accumulation of DNA lesions that promotes genomic instability (Yao and Dai, 2014). Cancer development is a multistep process and dysregulation of mechanisms that control DNA repair which further aggravates genomic instability due to uncontrolled cell growth, proliferation, differentiation, and apoptosis (Zhou et al., 2020).

Our genomes are under regular exposure to endogenous and exogenous genotoxic stress which results in DNA damage (Bernstein et al., 2013; Torgovnick and Schumacher, 2015). Endogenous genotoxic stress usually occurs via natural cellular processes such as transcription, replication, and recombination. Whereas exogenous genotoxic stresses occur via environmental factors like ultraviolet light, ionizing radiation, or exposure to cytotoxic or genotoxic chemicals (Chatterjee and Walker, 2017; Torgovnick and Schumacher, 2015). Damage to DNA can occur at a sequential level such as mismatch pairing or it can occur at a chromosomal level as either DNA single-strand breaks (SSBs) or DNA double-strand breaks (DSBs). The presence of DNA damage is a normal occurrence that is frequently repaired quickly and precisely. However, dysregulation of DNA repair pathways leads to halted DNA repair, resulting in large-scale chromosomal alterations like insertion, deletions, or translocations associated with increasing genomic instability essentially promoting cancer initiation and progression (Davis and Chen, 2013; Sharma and Misteli, 2013).

DSBs may be toxic when unrepaired or incorrectly repaired since this may result in chromosomal recombination or alterations. These contribute to genomic instability which is a hallmark of cancer (Davis and Chen, 2013). DSBs are breaks on both DNA strands causing large chromosomal aberrations and if these breaks remain unrepaired or are incorrectly repaired

these aberrations become detrimental as they create a strain on the DNA by interfering with one or more genes in that region and eventually lead to cell death, chromosomal alterations or loss of heterozygosity. These regions may include but are not limited to the enhancer, insulator, promotor, transcriptional activator/repressor regions, or non-coding regions. The accumulation of these lesions all contributes to genomic instability (Aleksandrov et al., 2020; Shrivastav et al., 2008; Zhang et al., 2021). DNA lesions occur throughout the cell cycle, and cells have checkpoints at each cell cycle stage to assess DNA quality. The signalling pathways that sense DNA damage i.e. DDR regulates the cell cycle and initiates the appropriate response. Depending on the degree of DNA damage and cell cycle stage, the cells will undergo cell cycle arrest and either DNA repair or apoptosis (Figure 1) (Iarovaia et al., 2014; Kavanagh et al., 2013).

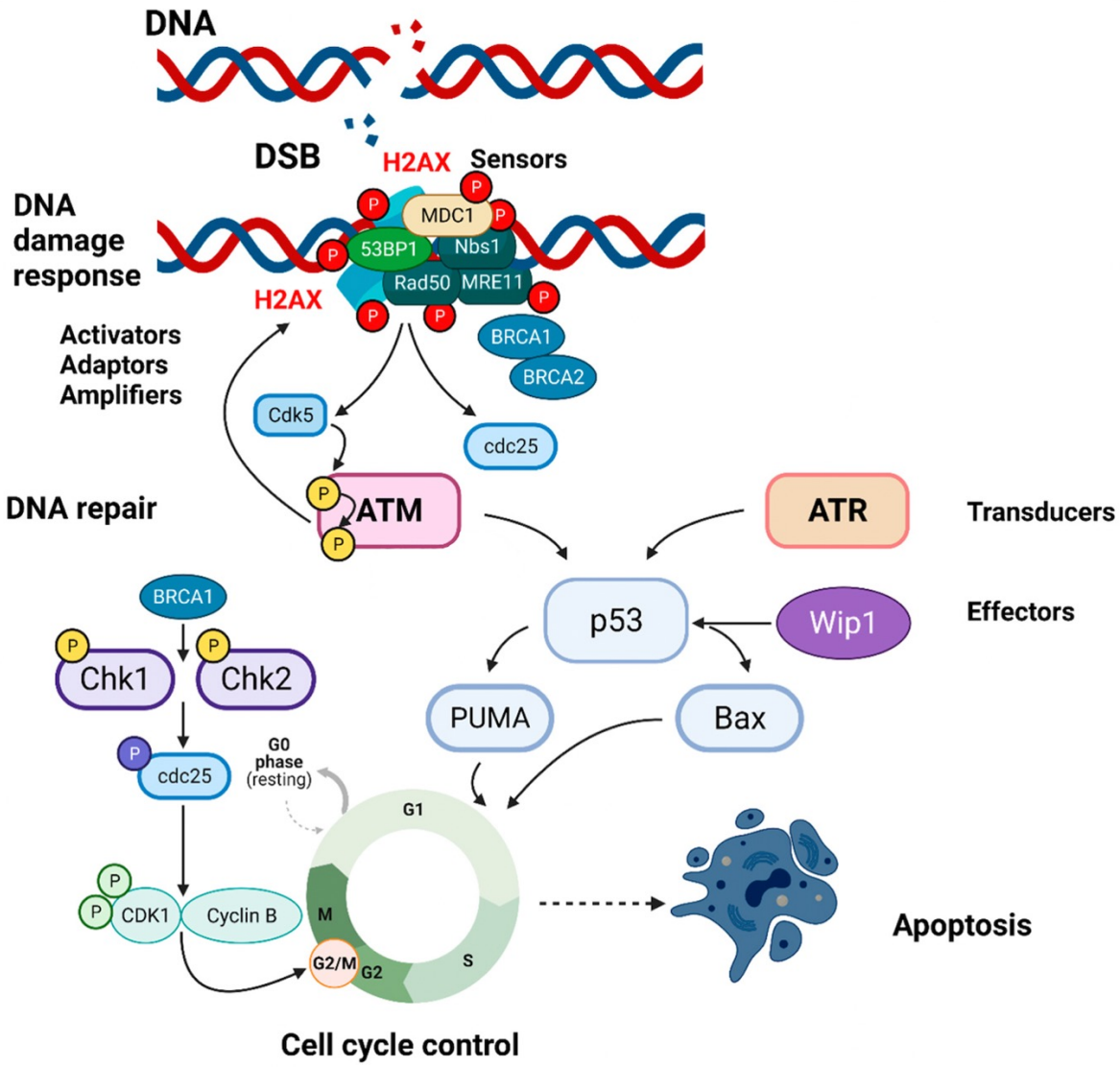

Figure 1: DNA damage response and signalling pathways in response to DNA double-strand breaks.

Initially, DNA DSBs are sensed by the Mre11-Nbs1-Rad50 (MRN) complex by binding to the DSB and initiates the DNA damage response pathway by activating the primary signalling kinases ATM, ATR and DNA-PK. In turn, this activates the phosphorylation of H2AX at ser139 (γH2AX). Upon binding to the DSB γH2AX binds to the sensor protein MDC1 which modifies the chromatin around the DSB to allow the DNA repair proteins access to the DSB. γH2AX and MDC1 recruits 53BP1 to process the DDR signal and recruit ATM and ATR to the DSB. The DNA repair proteins BRCA1, BRCA2, Rad50, Ku70/Ku80 and Artemis, and the checkpoint control proteins chk1, chk2 p53, and p21 are recruited to the DSB. Depending on the extent of the DNA cells will undergo cell cycle arrest followed by DNA repair or if the DNA damage is too extreme cells will undergo apoptosis. Image adapted from (Merighi et al., 2021).

1.2 The MRN Complex

Our genomes face several types of DNA damage regularly, these include the more frequently occurring DNA SSBs as well as the more lethal occurring DNA DSBs (Jackson and Bartek, 2009). There are various ways in which DSBs can occur, however, they more commonly emerge because of two closely located SSBs or while repairing other lesions (Jeggo and Löbrich, 2007). These lesions can be induced endogenously through DNA metabolising processes such as replication errors and uncontrolled recombination or through reactive oxygen species. They can also be induced exogenously via exposure to genotoxic or cytotoxic chemicals or environmental factors like ionizing radiation or ultraviolet light (Giglia-Mari et al., 2011). Unrepaired and incorrectly repaired DSBs are harmful as they lead to loss of chromosomes, altered chromosomal structures, lesions, or cell death. Since they occur through DNA replication and recombination, DSBs must be repaired constantly and accurately (Dudáš and Chovanec, 2004).

To sense and repair the damaged DNA frequently faced by our genomes, our cells activate the DDR signalling cascade (Jackson and Bartek, 2009; Sharma et al., 2015). There are three major processes involved in the DDR; first, the damaged DNA has to be detected, the second is to have mechanisms in place to regulate transcription and the cell cycle checkpoints and the last is to catalyse the repair mechanism of the damaged DNA. However, when the damage is too extensive DDR will signal for apoptosis of the damaged cell (Kavanagh et al., 2013). In the presence of DNA DSBs, the first step of DDR is sensing and recognising the damaged DNA. The MRN complex (meiotic recombination 11 homolog 1 (**M**re11) – DNA repair protein Rad50 (**R**ad50) – phosphopeptide-binding Nijmegan breakage syndrome protein 1 (**N**bs1) usually detects these DSBs and signals for the protein complexes required for repair (Figure 1) (Lamarche et al., 2010).

1.2.1 MRN in DSB Sensing

The MRN complex is a multi-domain complex consisting of two Mre11 subunits, two Rad50 subunits, and two Nbs1 subunits. These interact with each other to initially sense DSBs and bind to the DNA ends initiating DDR and signals for specific DNA repair factors (Lamarche et al., 2010; Syed and Tainer, 2018). The Mre11 nuclease dimer binds to chromatin when a DSB is recognised and forms the core of the MRN complex, which is important for MRN complex formation, as Mre11 binds directly to the DNA, Rad50, and Nbs1 subunits (Lamarche et al., 2010; Syed and Tainer, 2018).

The Mre11 subunits contain a Rad50-binding domain between the two DNA-binding domains (Qiu and Huang, 2021). Rad50 enables ATP binding to the MRN complex through the ATP-binding cassette (ABC)-ATPase. This cassette functions in unwinding DNA when ATP is hydrolysed in an Nbs1-dependent manner, thus enabling Mre11 to process DNA ends (Lamarche et al., 2010; Williams et al., 2007). Nbs1 contains a Mre11-interaction domain, whereby Mre11 binds, as well as two Breast cancer C-terminus (BRCT) and a forkhead-associated (FHA) domain domains. BRCT and FHA respectively bind to threonine and serine residues of phosphorylated DNA damage proteins and checkpoint proteins. This is crucial for the recruitment of other repair proteins such as Ataxia Telangiectasia mutated protein (ATM) to repair DSBs (Lamarche et al., 2010). Mre11, Nbs1, and Rad50 work together to sense DSBs, unwind the DNA, and recruit DNA damage-associated proteins such as Breast Cancer Susceptibility protein 1 and 2 (BRCA1 and BRCA2), Rad51, Ku70, and Ku80 (Ku70/Ku80 heterodimer) and Artemis, repair proteins and cell cycle checkpoint proteins, checkpoint control proteins checkpoint kinase 1(Chk1), checkpoint kinase 2(Chk2), p53 and p21 to DSB sites (Kavanagh et al., 2013).

The MRN complex is one of the initial responders of DNA DSBs and is vital for sensing and responding to DNA DSBs (Bian et al., 2019; Lamarche et al., 2010). In the presence of DSBs, MRN binds to the DSBs site before DNA repair pathway choice is determined. Once bound, MRN initiates DNA end resection where the Mre11 endonuclease makes an incision generating a 3′ ssDNA overhang (Kavanagh et al., 2013; Qiu and Huang, 2021; Zhao et al., 2020). MRN then activates the primary signalling kinases (ATM, ATM, and Rad3-related kinase (ATR) and DNA Protein Kinase (DNA-PK) (Figure 1) that regulate the DSB response signalling, and in turn the histone H2AX is phosphorylated at Ser139 (γH2AX) (Kavanagh et al., 2013).

1.2.2 H2AX Phosphorylation Signalling

Phosphorylation of histone H2AX on Ser139 (γH2AX), an early DSB marker, is crucial for DNA repair as it amplifies DDR signalling and alters chromatin structure in the vicinity of the DSB by binding to the mediator of DNA damage checkpoint protein 1 (MDC1). This results in the unfolding of the chromatin structure allowing DNA repair proteins access to the DSB (Aleksandrov et al., 2020; Nikolova et al., 2014; Podhorecka et al., 2010; Ricoul et al., 2019). In the presence of a DSB γH2AX is rapidly phosphorylated by one of the phosphoinositide 3-kinase-related protein kinases (PIKK). For example, in the homologous recombination (HR) pathway, γH2AX is phosphorylated by ATM whereas, in response to hypertonic cellular conditions, γH2AX is phosphorylated by DNA-PK. DNA fragmentation resulting from apoptosis or non-Homologous end joining (NHEJ), excessive presence of SSBs, or DNA replication stress results in phosphorylation of H2AX by ATR (Aleksandrov et al., 2020; Kavanagh et al., 2013; Podhorecka et al., 2010). MDC1 is recruited and binds to γH2AX upon phosphorylation of the histone, this recruits MRN and ATM to the DSB site further enhancing the ATM signal to recruit and activate downstream DDR proteins that regulates the cells fate (Salguero et al., 2019; Stucki and Jackson, 2006).

γH2AX and MDC1 accumulate at the DSB sites to amplify the DSB signal initiated by the MRN complex and is also a docking site for downstream DDR repair proteins (Salguero et al., 2019). γH2AX and MDC1 recruit the mediator protein p53 binding protein (53BP1) to process the DDR signal and recruit ATM and ATR to the DSB sites which colocalize with γH2AX. In turn, this recruits the required DNA repair proteins, BRCA1, BRCA2, Rad51, Ku70/Ku80 heterodimer, and Artemis, as well as the checkpoint control proteins Chk1, Chk2, p53, and p21 (Figure 1). These proteins work together to activate cell cycle arrest; the checkpoint proteins Chk1 and Chk2 activate the tumor suppressor p53 which in turn activates p21 essentially arresting cell cycle progression, allowing either repair of the DSB or activation of apoptotic pathways if the extent of DNA damage is too extreme (Eren et al., 2021; Kavanagh et al., 2013; Lamarche et al., 2010).

1.3 DNA DSBs Repair

After the MRN complex initially senses DSBs and signals for H2AX phosphorylation, either the homologous recombination (HR) or non-homologous end joining (NHEJ) repair pathway is initiated (Mao et al., 2008; Shrivastav et al., 2008). Most DNA DSBs are repaired via the

error-prone and cell cycle-independent NHEJ that occurs at a quicker and more frequent rate (Chang et al., 2017; Lieber, 2010). Alternatively, the cell cycle-dependent HR repair pathway requires a homologous strand as a template for DNA repair confining HR to the late S phase and G2 phase of the cell cycle (Johnson and Jasin, 2000; Krajewska et al., 2015). The mechanism of DNA repair initiated is dependent on the cell cycle stage. While DNA repair via NHEJ occurs throughout the cell cycle, HR is favoured during the late S/G2 phase of the cell cycle when the homolog is nearby, therefore, cells require mechanisms in place to assist in pathway choice when HR repair is available (Lieber, 2010).

During the S/G2 cell cycle phase, NHEJ and HR repair pathway choice is determined by the 3′ ssDNA generated. 53BP1 and BRCA1 compete at the DSB ends to either protect the DNA favouring NHEJ repair or resect the DNA ends favouring HR repair (Han and Huang, 2020). In the initial stages of DSB sensing 53BP1 is recruited to the DSB to process the DDR signal and protect the DNA ends from resection. 53BP1 recruits Pax transactivation domain-interacting protein (PTIP) that recruits the nuclease Artemis to remove the short regions of the DNA ends, and Rap1-interacting protein (RIF1) to protect the DNA ends (Han and Huang, 2020; Swift et al., 2021; Wang et al., 2014). Whereas BRCA1 is recruited to the DSB after 53BP1 and competes with the DNA end protection activity by displacing 53BP1 to allow BRCA1 to bind to the DSB ends to promote DNA end resection and HR repair (Han and Huang, 2020). 53BP1 is dislodged from the DSB site by specificity protein 1 (Sp1), a transcription factor, that binds to the DSB early in DDR sensing and recruits 53BP1 essentially promoting NHEJ repair but when phosphorylated by cyclin dependant kinase 2 (CDK2) early in the S phase of the cell cycle, Sp1 behaves as a molecular switch that initiates the change from NHEJ to HR by dislodging itself and 53BP1 to allow BRCA1 to bind to the DNA ends and initiating HR repair (Swift et al., 2021). Other factors such as the cell cycle phase and the structure of the DNA ends of the DSB also assist in regulating DNA end resection and contribute to DNA repair by either NHEJ or HR (Han and Huang, 2020).

1.3.1 Non-Homologous End Joining

Aligning the microhomologous sequences of the damaged DNA ends mediates NHEJ repair which may involve one or multiple complementary bases. Short regions of the 3′ or 5′ overhangs are removed from the damaged DNA ends by either endonuclease or exonucleases to produce short microhomologous regions which may lead to minor insertions or deletions

(Chang et al., 2017; Sfeir and Symington, 2015; Shrivastav et al., 2008). The Ku70/Ku80 heterodimer binds to the DSB site forming the Ku:DNA complex, and recruits and holds the required polymerases, nucleases, and ligases during repair (Lieber, 2010).

The DNA-dependent protein kinase catalytic subunit (DNA-PKcs) complex is recruited to the DSB by the Ku70/Ku80 heterodimer where it phosphorylates itself and the nuclease Artemis required for DNA end processing (Han and Huang, 2020). DNA-PKcs, which have various nuclease activity (5′ endonuclease and exonuclease activity and 3′ endonuclease activity), bind to the Ku:DNA complex and together with Artemis cut different types of damaged DNA overhangs to remove the damaged DNA. DNA-PKcs and Artemis work together with pol μ and pol l (DNA polymerase mu and lambda) to first discharge the damaged DNA and then add nucleotides in either a template-dependant or template-independent manner (Davis and Chen, 2013; Lieber, 2010; Shrivastav et al., 2008). Finally, once the DNA is repaired by DNA ligase IV, the scaffolding proteins X-ray cross-complementing protein 4 (XRCC4) and XRCC4-like factor (XLF), and the paralog of XRCC4 and XLF (PAXX) form the ligase complex that is recruited and binds to the Ku:DNA complex, and ligates the gaps and the incompatible DNA ends (Han and Huang, 2020; Lieber, 2010).

1.3.2 Homologous Recombination

HR repair is initiated by 5′ - 3′ DNA end resection through C-terminal binding protein 1 (CtBP) interacting protein (CtIP), BRCA1, and MRN interaction (Han and Huang, 2020). Following MDC1 binding at the DSB site, the receptor-associated protein 80 (Rap80) is recruited, in turn, Rap80 recruits BRCA1 to the DNA ends. In the S/G2 phase of the cell cycle, DNA end resection is activated by BRCA1 interacting with MRN and its co-factor CtIP to process the DNA ends to produce long 3′ ssDNA overhangs (Batenburg et al., 2019; Han and Huang, 2020; Li et al., 2017). The replication protein A (RPA) coats and protects the 3′ ssDNA overhangs to prevent the DNA overhangs from folding back on themselves, to regulate DNA end resection, and protect the ssDNA from nucleases (Chen et al., 2013; Soniat et al., 2019).

HR repair consists of related pathways that work together and uses a homologous template strand, normally the sister chromatid, for homology-directed repair of the DSBs. RPA coating the ssDNA is then displaced by the accessory proteins BRCA2 and Rad51, and the Rad51 recombinase binds to the ssDNA ends to form the nucleoprotein Rad51-ssDNA strand (Han

and Huang, 2020; Li et al., 2019). The Rad51-ssDNA strands track down the homologous DNA sequence and initiate DNA strand invasion to form the displacement loop (D-loop), a triple-stranded DNA structure. DNA synthesis is then initiated using the 3′ end of the homologous DNA sequence and HR repair is completed by re-ligating the newly recombinant DNA (Han and Huang, 2020; Ma et al., 2017).

Following DNA repair completion γH2AX is dephosphorylated by the oncogenic Wild-type p53- Induced Phosphatase 1 (WIP1) allowing the chromatin to return to its unwound form (Eren et al., 2021; Moon et al., 2010). The p53-activated protein phosphatase WIP1 is a serine/threonine phosphatase that regulates stress in the DDR pathway by dephosphorylating γH2AX and the proteins Chk1, Chk2, ATM, p53, and other proteins phosphorylated by ATM, ATR, and DNA-PK early in DDR (Macůrek et al., 2010; Moon et al., 2010). Dephosphorylation of the DDR-activated proteins Chk1, Chk2, and p53 stabilizes p53 preventing p21 expression and allowing re-entry into the cell cycle and cell cycle progression. Furthermore, dephosphorylation of γH2AX suppresses activation of the DDR-activated protein, ceasing DDR and DNA repair pathways and allowing the chromatin to return to its folded structure once the DNA is repaired (Eren et al., 2021; Macůrek et al., 2010; Moon et al., 2010).

1.4 LncRNAs Regulate DDR and Genomic Stability

Long non-coding RNAs (lncRNAs) are regulatory non-coding RNAs (ncRNAs), 200 or more nucleotides in length, that have been suggested to be an extensive driver of carcinogenesis. LncRNAs resemble messenger RNA (mRNA), in that they are also transcribed by RNA polymerase II, are polyadenylated and some lncRNAs are capped. Additionally, lncRNAs do not have an open reading frame (ORF) and are unable to code for proteins (Prensner and Chinnaiyan, 2011). However, lncRNAs have fewer exons and are less stable (Tehrani et al., 2018). LncRNAs are arranged into five classes depending on their position in the genome concerning protein-coding regions. First are the lncRNAs transcribed from the promoter of a protein-coding gene, termed bidirectional lncRNAs, as it transcribes the lncRNA in the opposite direction of the protein gene and has a transcription start site that is less than 1 kb from the protein-coding start site. The second is the lncRNAs located only in the intron regions of the protein-coding genes, termed intronic lncRNAs. The lncRNAs that are positioned between protein-coding genes that can be transcribed in either direction are called intergenic

lncRNAs. The sense lncRNAs are lncRNAs that overlap with one or more of the introns or exons of the protein-coding genes on the sense RNA strand they are located on. Last are the antisense lncRNAs transcribed from the protein-coding region of antisense RNA (Balas and Johnson, 2018; Latgé et al., 2018). LncRNAs regulate DDR and genomic stability due to their oncogenic or tumor suppressive functions and have been suggested to play crucial roles in biological functions, such as chromatin remodeling, transcriptional regulation, and mRNA editing and splicing (Thapar, 2018; Zhang et al., 2016).

LncRNAs bind to chromatin-modifying complexes, histones, and transcription factors by forming three-dimensional structures that allow these lncRNAs to function in gene regulation, transcription, and post-transcriptional processes by mediating RNA-DNA interactions, RNA-RNA interactions, and RNA-protein interactions (Figure 2) (Ling et al., 2015; Schmitt and Chang, 2016; Tehrani et al., 2018). LncRNAs play a role in chromatin modifications by mediating RNA-protein interactions. LncRNAs interact with DNA modifying enzymes or histone modifying enzymes, such as the histone methyltransferase Polycomb Repressive Complex (PRC), DNA methyltransferases (DNMTs), and histone demethylase, by either binding directly to these DNA and histone modifying enzymes and acting as a chaperone for chromatin modifiers or the lncRNAs integrate themselves into the chromatin-modifying complexes acting as a scaffold for chromatin modification complexes (Ferrè et al., 2016; Han and Chang, 2015; Jalali et al., 2015). LncRNAs also interact with DNA binding proteins such as enhancers, promoters, and insulators, that have multiple transcription factor binding sites, by either recruiting or dislodging transcription factors to regulate gene expression (Das et al., 2020; Long et al., 2017). LncRNAs mediate RNA-RNA interactions where they may have a role in mRNA processing events such as mRNA capping, mRNA editing, or splicing. LncRNAs may also interact with mRNA and regulate its stability or degradation at a post-transcriptional level, (Fang and Fullwood, 2016; Hadjicharalambous and Lindsay, 2019). This suggests that lncRNAs play important roles in epigenetic regulation, gene expression integrity, imprinting, chromatin remodeling, and transcription and post-transcriptional processes (Hadjicharalambous and Lindsay, 2019; Tehrani et al., 2018).

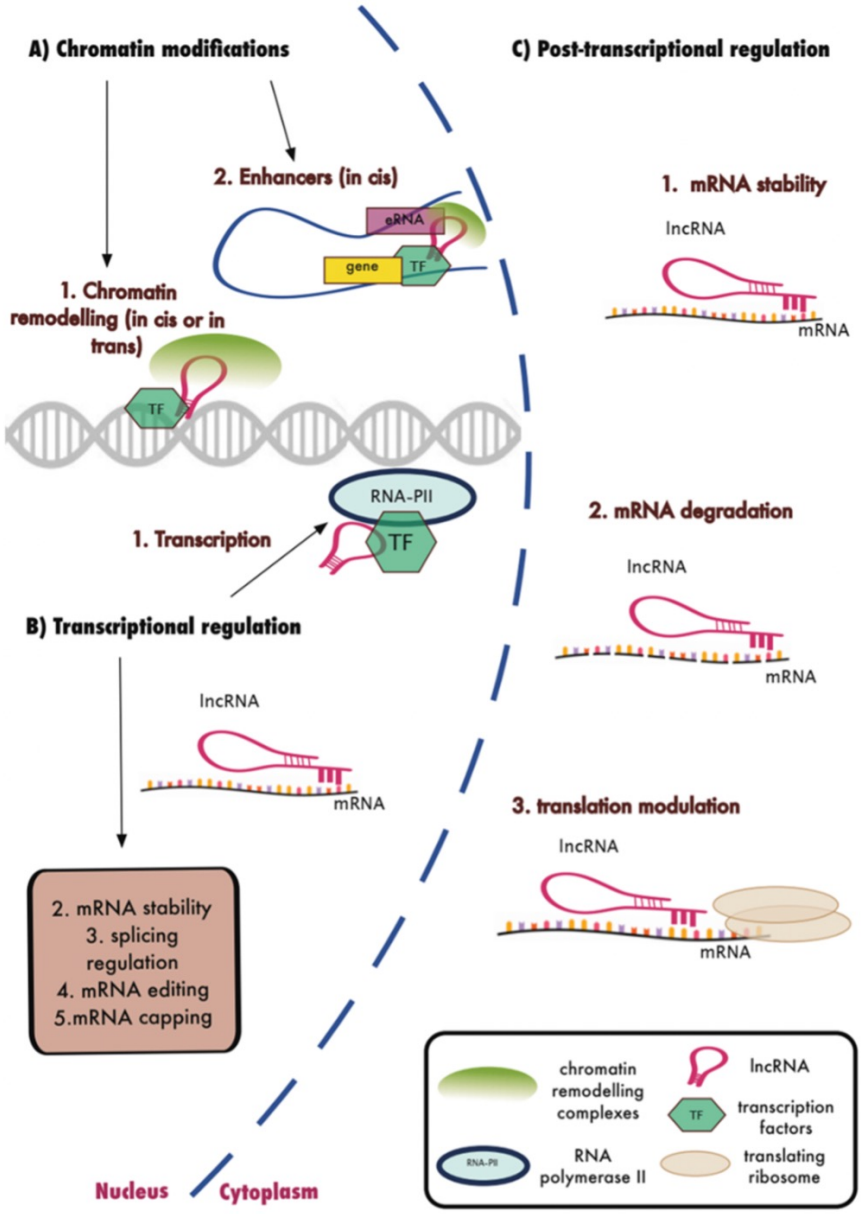

Figure 2: Biological functions of lncRNAs.

LncRNAs regulate gene expression by interacting with protein-coding genes and their mRNA transcripts. (A) LncRNAs regulate gene expression by interacting with chromatin remodeling complexes and transcription factors. (B) Transcription and RNA processing events are also regulated by lncRNAs. (C) LncRNAs regulate post-transcriptional events involved in mRNA stability and mRNA degradation and also regulate the translation of mRNAs (Hadjicharalambous and Lindsay, 2019).

LncRNAs regulate gene expression through various molecular pathways, many of which are related to cancer initiation and progression when their expression is dysregulated (Huarte, 2015). Functional mutations in the DNA transcripts that code for lncRNAs result in the lncRNA being over-expressed or under-expressed, although, many lncRNAs are over-expressed in

cancer because of their low expression in healthy cells and their capability to regulate cancer-related pathways (Calin et al., 2007; Gupta and Tripathi, 2017). For example, breast cancer metastasis is stimulated when the lncRNA HOX antisense intergenic RNA (HOTAIR) silences genes involved in the homeobox D(HOXD) cluster that is important for growth and development (Huarte, 2015; Schmitt and Chang, 2016). Therefore, functional mutations in lncRNAs that participate in these molecular pathways and whose dysregulation contributes to cancer hallmarks can be used as therapeutic targets (Huarte, 2015; Schmitt and Chang, 2016).

The lack of appropriate diagnostic biomarkers has resulted in cancer being one of the leading causes of death worldwide. Many cancers are associated with dysregulated lncRNA expression and identifying their differential expression is critical in cancer diagnosis (Gupta and Tripathi, 2017; Tehrani et al., 2018). The study by Sun et al. (2019) has identified that the upregulation of the lncRNAs Colorectal Neoplasia Differentially Expressed (CRNDE), H19, Urothelial carcinoma associated 1 (UCA1), and HOTAIR contribute to colorectal cancer development, proliferation, invasion and migration and is also largely associated with chemoresistance. Therefore, these lncRNAs can be used as a predictive biomarker for treatment sensitivity and tumor prognosis in colon cancer patients. LncRNAs are tissue-specific and dysregulated in many cancers and their expression is specific in certain cancers. This makes lncRNAs useful markers of prognosis, valuation, and diagnosis of treatments in response to multiple cancers (Tehrani et al., 2018; Yarmishyn and Kurochkin, 2015). LncRNA studies have been moving towards the emerging roles of lncRNAs in regulating multiple DDR signalling pathways, such as the ATM and ATR pathways and the p53 pathways. The lncRNAs PANDA, ANRIL, and DDSR1 that were studied in this project are involved in DDR signalling and are described below.

1.4.1 LncRNA PANDA

The antisense lncRNA p21 associated ncRNA DNA damage activated (PANDA) of the cyclin-dependent kinase inhibitor 1A (CDKN1A) and is p53 regulated. PANDA has a 5'-cap, is polyadenylated, non-spliced, and is located on the p21 locus about 5 kb upstream of CDKN1A. PANDA expression is p53-induced and this lncRNA plays a role in DNA damage signalling, cell cycle regulation, and apoptosis (Peng et al., 2017; Shi et al., 2019). The lncRNA PANDA and the polycomb repressive complexes 1 and 2 (PRC1 and PRC2) bind to the scaffolding protein scaffold-attachment-factor A (SAFA) in proliferating cells to repress the senescent

activating genes which include p21. Additionally, the transcription factor E2F Transcription Factor 1 (E2F1), which regulates the expression of cell cycle progression genes, is activated and expresses the nuclear transcription factor Y subunit alpha (NF-YA)-dependant proliferation genes such as cyclinD1 and cyclinD2. However, in senescent cells when SAFA expression is reduced PANDA binds to NF-YA and inhibits activation of E2F1 preventing activation of proliferation genes usually activated by NF-YA (Lettieri-Barbato et al., 2022; Manickavinayaham et al., 2020; Puvvula et al., 2014).

The CDKN1A locus and lncRNA PANDA are co-regulated by the p53 transcription factor (Su et al., 2018). CDKN1A, which encodes the cell cycle inhibitor p21, and PANDA have a p53 binding site located between the CDKN1A locus and the DNA encoding PANDA. In the presence of DNA, damage p53 co-regulates the transcriptional activation of both CDKN1A and PANDA in a bi-directional manner. CDKN1A activates the cell cycle inhibitor p21 which arrests the cell cycle and NF-YA interacts with PANDA to repress the expression of the pro-apoptotic genes for damage (NOXA) and p53 upregulated modulator of apoptosis (PUMA) to promote cell-cycle arrest and cell survival (Imbriano et al., 2012; Su et al., 2018).

PANDA plays crucial roles in regulating cellular senescence pathways required to determine the fate of cells when faced with DNA damage. Cellular senescence is a response mechanism activated when cells are under stress, depending on the extent of DNA damage cells would need to undergo cell cycle arrest, DNA repair, or cell death (Kumari and Jat, 2021; Puvvula, 2019). In proliferating cells PANDA functions in regulating proliferation by binding to SAFA, PRC1, and PRC2 forming a repressor complex that negatively regulates CDKN1A expression. CDKN1A encodes the cell cycle inhibitor p21 and when repressed, E2F1 is activated which in turn activates the pro-apoptotic genes cyclinD1, cyclinD2, cyclinE1, and Bcl-2 expression resulting in proliferation (Puvvula et al., 2014; Shi et al., 2019). Alternatively, in cells undergoing senescence, PANDA expression is increased, allowing PANDA to act as a molecular decoy that sequesters NF-YA. Upon binding to NF-YA, E2F1 is inhibited, this, in turn, activates CDKN1A expression which inhibits cyclinD1, cyclinD2, cyclinE1, and Bcl-2 expression promoting apoptosis (Puvvula et al., 2014).

1.4.2 LncRNA ANRIL

The antisense non-coding RNA in the INK4 locus (ANRIL) is encoded on the 9p21 chromosome, a region well known for disease-associated polymorphisms. ANRIL is located at the cyclin-dependent kinase inhibitor 2A/B (CDKN2A/B) (also known as INK4-ARF) locus where CDKN2A encodes for the spliced variants p16 (INK4A) and p14 (ARF), and CDKN2B encodes p15 (INK4B) proteins (Congrains et al., 2013). CDKN2A is located near the first ANRIL exon and CDKN2B is located within the first ANRIL intron. ANRIL is transcribed from the same locus in the antisense direction of CDKN2A in response to DNA damage and recruits PRC1 and PRC2 to repress the INK4A-ARF-INK4B locus (Kong et al., 2018; Meseure et al., 2016).

ANRIL is induced in an ATM-E2F1-dependent manner and represses the tumor suppressor genes INK4A, ARF, and INK4B (Popov and Gil, 2010). ANRIL has an E2F1 binding element in its promotor region that assists in activating ANRIL downstream of the ATM-ATR signalling pathway in response to DNA damage (Wan et al., 2013). Activation of ANRIL recruits the PRC1 and PRC2 proteins to the INK4 locus where it silences the INK4A-ARF-INK4B locus by forming heterochromatin around it thus repressing the INK4A-ARF-INK4B function and inhibits CDK4 and CDK6 expression which in turn prevents the activation and phosphorylation of the retinoblastoma protein (pRB) and p53, that when activated promotes apoptosis (Popov and Gil, 2010; Subramanian et al., 2013). Therefore, ANRIL contributes to cell cycle regulation by regulating INK4A-ARF-INK4B expression and promotes cell cycle arrest in response to DNA damage.

1.4.3 LncRNA DDSR1

The lncRNA DNA damage sensitive RNA1 (DDSR1) was first identified by Sharma et al (2015) who noticed that in response to DNA damage DDSR1 expression was upregulated. In response to DSBs ATM is activated by MRN at the DSB site, in turn, ATM activates a nuclear cascade of kinases one of which is the transcription factor Nuclear factor kappa-B (NF-kB) (Habraken and Piette, 2006). DDSR1 is activated in an ATM-NF-kB-dependent manner, independent of the transcription factor p53, at the DNA ends of the DSB site and assists in regulating the DDR signalling molecules γH2AX; RPA and chk1and are induced early on in response to DNA damage to promote HR repair. DDSR1 regulates these signalling molecules

by interacting with the BRCA1 susceptibility protein to promote DNA end resection, thus favouring the HR repair pathway (Sharma et al., 2015).

DDSR1 interacts with heterogeneous nuclear ribonucleoprotein U-like protein 1 (hnRNPUL1) and BRCA1 in the early stages of DDR to regulate DNA end resection and promote DSB signalling and repair (Sharma et al., 2015). The BRCA1 and receptor-associated protein 80 (Rap80) complex is recruited to DSB sites early in DDR signalling and copious amounts of BRCA1 and Rap80 binding to DSB ends restricts DNA end resection, therefore, cells have put mechanisms in place to control BRCA1 and Rap80 binding at these sites. The MRN complex then recruits RNA binding protein hnRNPUL1 to the DNA ends where it interacts with DDSR1 to regulate BRCA1 and RAP80 binding at DSB ends which in turn initiates a DDR signalling cascade that arrests the cell cycle to allow for DNA repair to take place (Polo et al., 2012; Sharma et al., 2015).

1.5 NaCl-Induced DNA Damage

Tonicity levels are well regulated in cells, however, normal cells are more sensitive to hypertonic environments compared to cancer cells (Argyropoulos et al., 2016; Miermont et al., 2019). Biological mechanisms, such as osmotic pressure and mechanical stretching, are well regulated by cellular homeostasis and its microenvironment (Fan et al., 2021). Under normal cellular conditions, cells maintain the intracellular volume of solutes and water, when Na^+ levels are increased, i.e., cells are placed in hypertonic media, cells dispel their intracellular water and solutes to assist in maintaining its osmotic pressure gradient resulting in cell shrinkage as a mechanism of survival (Argyropoulos et al., 2016; Stöhr and Rehm, 2021). As a result of cell shrinkage and nuclear water loss, proteins are either degraded or translocated to the cytoplasm. Hypertonic stress affects the protein structure by unfolding the protein and exposing its usually covered hydrophobic regions of proteins. In turn, the protein folds back on itself and forms protein aggregates eventually degrading the protein (Burkewitz et al., 2011). However, not all proteins are degraded, some nuclear proteins are transiently recruited to the cytoplasm via nucleocytoplasmic shuttling, preventing their function (Hock et al., 2018). Non-cancer cells have limited function in hypertonic environments due to cell shrinkage, whereas cancer cells are suggested to have better osmoregulatory mechanisms in place that assist in keeping cellular processes such as mitosis and DNA repair active (Miermont et al., 2019).

Initiation of DDR is proposed to be hindered in response to high sodium chloride (NaCl) concentrations essentially resulting in transiently arresting all cell cycle progression (Dmitrieva et al., 2011). Under normal cellular conditions, cells respond by repairing the DNA and re-entering the cell cycle, however, under hypertonic cellular conditions cells are unable to repair these lesions before re-entering the cell cycle (Burg et al., 2007). Cells placed in high NaCl conditions result in the translocation of most DNA repair proteins and complexes out of the nucleus and into the cytoplasm to maintain cell survival. In particular, Mre11 normally located in the nucleus is sequestered in the cytoplasm under high NaCl conditions, where it is unable to sense DSBs and initiate DDR, due to signalling and repair being disrupted, this in turn prevents the phosphorylation of histone H2AX also required for DNA repair resulting in the accumulation of DSBs located in gene deserts along the nuclear periphery (Burg et al., 2007; Dmitrieva et al., 2011, 2003; Dmitrieva and Burg, 2008). The nuclear periphery is composed of transcriptionally inactive heterochromatin and the non-coding regions of DNA are predominantly located in gene deserts that are rich in regulatory genes and have a high frequency of repetitive regions (Shopland et al., 2006; Touceda-Suárez et al., 2020). High NaCl concentrations result in the accumulation of less toxic DSBs mostly located in gene deserts.

Hypertonic stress results in transient cell cycle arrest giving cells time to activate adaptive mechanisms initiated by the signal transduction kinase stress-activated protein kinase (SAPK) that assists cells in regulating metabolism, gene expression, and cell cycle progression (Duch et al., 2012). In response to osmotic stress, SAPK regulates several phases of the cell cycle to prevent DNA repair. The study by Dmitrieva et al. (2011) showed that the cells adapted to high NaCl levels after a few hours and would begin to proliferate again, however, DDR was not activated and the DSBs were still present in the cells. When placed in hypertonic environments cells enter an osmoprotective state regulated by the tonicity-responsive transcription factor nuclear factor of activated T cells-5 (NFAT5) involved in regulating cellular homeostasis under hypertonic environmental stresses (Lee et al., 2019). The mitogen-activated protein kinases (MAPKs) activate multiple genes that are involved in proliferation, apoptosis, and differentiation. In hypertonic environments MAPKs activate several genes and some of these genes are also activated through NFAT5 response. NFAT5 activates the genes that protect the cell and activates the genes that assist the cell in adapting to hyperosmotic stress, and the genes involved in DNA repair are inhibited. Therefore, when cells re-enter the cell cycle, DNA repair is not activated leading to DSB accumulation (Burg et al., 2007; Casali et al., 2018; Izumi et al., 2015; Kumar et al., 2020).

Reduced NaCl concentrations allowed DDR to be activated once again and the DSBs were rapidly repaired (Dmitrieva et al., 2011). The study by Dmitrieva et al. (2003) showed the nuclear translocation of Mre11 in response to NaCl withdrawal, in turn, the MRN complex formed and could bind to the DSB, and signals for the required DNA repair factors such as phosphorylation of the histone H2AX. γH2AX accumulates and amplifies the DSB signal which then activates the downstream DNA repair proteins allowing the cells to continue through the cell cycle once again. This suggests when hypertonicity levels are reduced, DNA repair recommences (Dmitrieva et al., 2003).

NaCl is a useful agent to study DDR due to the translocation of Mre11 to the cytoplasm in high NaCl concentrations resulting in transient cell cycle arrest and inhibited DNA repair. Inhibited DNA repair can be observed by reduced γH2AX expression and following NaCl withdrawal Mre11 translocated to the nucleus, forms the MRN complex which binds to the DSB and allows for the rapid formation of γH2AX, whose phosphorylation is accompanied by the progression of the cell cycle (Dmitrieva et al., 2003).

In this study, hypertonic media was used to promote DSB accumulation and prevent DNA repair. Cells were observed in the presence of NaCl and five minutes after NaCl withdrawal. Mre11 localisation, γH2AX levels, and lncRNA expression were observed in the presence of NaCl and immediately after NaCl withdrawal. Additionally, these effects were compared between cancer and non-cancer cell line.

2 Aims and Objectives

2.1 Aims

To investigate whether DNA damage associated lncRNA expression is altered in response to high NaCl in HEK293 and HT29 cells.

2.2 Objectives

2.2.1. To determine the concentration of NaCl that induces cell death in HEK293 and HT29 cell lines by MTT assay.

2.2.2. To observe Mre11 localisation after NaCl withdrawal in HEK293 and HT29 cells using confocal microscopy.

2.2.3. To quantify double-strand breaks after NaCl treatment by western blot for γH2AX in HEK293 and HT29 cells.

2.2.4. To observe the expression of lncRNAs PANDA, ANRIL, and DDSR1 during DDR signalling induced by NaCl in HEK293 and HT29 cells.

3 Methods

3.1 Lab Reagents

Chemicals and reagents were all purchased from Sigma-Aldrich unless otherwise stated.

3.2 Cell Culture

In this study two cell lines were used, HEK293, an immortalized human embryonic kidney cell isolated from a healthy female fetus that was terminated was used as a non-cancer control (Russell et al., 1977). The second HT29 cell line, isolated from a primary tumor of a 44-year-old Caucasian female with colorectal adenocarcinoma, was used as a cancer cell line. Both cell lines ("HT-29: Human Colorectal Adenocarcinoma Cell Line (ATCC HTB-38) | Memorial Sloan Kettering Cancer Center," n.d.) were grown and maintained in 1x DMEM/F-12 (1:1 Dulbecco's modified Eagle's medium and Hams F-12 nutrient mixture) and supplemented with 1% penicillin-streptomycin and 10% fetal bovine serum (FBS) (cell culture medium) in a 37 °C and 5% CO_2 incubator.

3.3 MTT Assay

To quantify cell viability in response to high NaCl exposure, the metabolic activity in HEK293 and HT29 cell lines was measured by the colorimetric 3-(4,5-dimethylthiazol-2-yl)-2,5-diphenyltetrazolium bromide (MTT) assay. First, cells were seeded into 96-well microplates at a concentration of $6x10^4$ cells/well in culture medium followed by incubation at 37 °C and 5% CO_2 for 24 hrs to allow cells to settle. The old medium was aspirated and HEK293 and HT29 cells were treated with 10 half dilutions from 0 – 2000 mM in fresh cell culture medium and incubated for 24 hrs at 37 °C and 5% CO_2. The medium was then aspirated and the working MTT solution (5 mg/ml MTT stock was prepared in 1x phosphate-buffered saline (PBS) and then diluted 1/10 in cell culture medium prior to the assay) was added to each well and the plates were incubated at 37 °C and 5% CO_2 for a further 2.5 hrs. After the MTT incubation, the medium was aspirated from all wells and dimethyl sulfoxide (DMSO) was added to each well to solubilise the purple formazan precipitate. This was then incubated at 37 °C and 5% CO_2 for 5 mins and then at room temperature in the dark for a further 25 min with gentle agitation. The

absorbance was measured at 570 nm. Sigmoidal curves were constructed using CurveExpert Basic software. The EC50 and EC30 values were determined using the equation $y = \alpha + \frac{\theta x^{\eta}}{\kappa^{\eta} + x^{\eta}}$, where α is the absence of NaCl, θ is the max subtract the min effect, η is the Hill exponent and κ is the EC50.

3.4 Confocal Microscopy

Confocal microscopy was used to visualise Mre11 localisation. HEK293 and HT29 cells were seeded in 6-well plates containing autoclaved coverslips cell culture medium was added to each well. Cells were incubated for 24 hrs to allow cells to attach to the coverslips and reach 60 – 70% confluency. Cells were either untreated or treated for 6 hrs (EC50) and 24 hrs (EC30) with NaCl, each followed by a 5 min NaCl withdrawal, and fixed to coverslips for 15 min in 3% formaldehyde in 1x PBS at room temperature on a shaker (60 rpm). The cells were then rinsed three times with 1x PBS for 5 min each on a shaker (90 rpm) and permeabilized with 0.5% Triton-X 100 in 1x PBS for 15 min at room temperature with shaking (60 rpm). The cells were washed 3 times for 5 min each on a shaker (90 rpm) followed by blocking the cells with 0.5% Bovine Serum Albumin (BSA) in 1x PBS for 30 min at room temperature on a shaker (60 rpm), followed by one rinse in 1x PBS for 5 min on a shaker (90 rpm). Primary antibody (MRE11 – Mouse monoclonal antibody, Santa Cruz) diluted in fresh 0.5% BSA in 1x PBS (1/200) was then added to each well and incubated in a moist container overnight on a shaker (60 rpm) at 4 °C (Controls included were primary antibody only and secondary antibody only). The cells were rinsed three times with fresh 0.5% BSA in 1x PBS with shaking (90 rpm) for 5 min each. Secondary antibody conjugated to FITC (M-IgGκ BP-FITC, anti-mouse monoclonal antibody (Santa Cruz)) diluted in fresh 0.5% BSA in 1x PBS (1/600) was added and incubated at room temperature in a moist container for 2 hrs. This was followed by rinsing with 1x PBS in the dark five times for 5 min each on a shaker (90 rpm). The cells were then counterstained with 0,06 µg/ml 4′,6-diamidino-2- phenylindole (DAPI) in 1x PBS in the dark on a shaker (60 rpm) for 5 min and were then rinsed with 1x PBS in the dark for five times on a shaker (90 rpm) for 5 min. Coverslips with cells were mounted using fluoromount mounting medium onto clean slides and stored at 4 °C in the dark until needed. Slides were viewed using the confocal microscope at the Life Science imaging Facility at Wits Medical school.

3.5 Western Blot

To quantify DSB formation and repair in HEK293 and HT29 cells western blot analysis for γH2AX was used.

3.5.1 Cell Treatment

HEK293 and HT29 cells were used in this study. Cells were treated with EC30 concentrations of NaCl for 4 hrs or 6 hrs, with or without 5 min NaCl withdrawal. Untreated cells were used as negative controls.

3.5.2 Protein Extraction and Quantification

Cells were lysed in 1x RIPA (50 mM Tris-HCl pH 8, 150 mM NaCl, 0.1 % SDS, 1% Triton X-100, 0.5 % sodium deoxycholate and 1 mM Ethylenediaminetetraacetic acid (EDTA), protease inhibitors used were: 1 mg/ml leupeptin, 0.5 M sodium fluoride, 0.1 M sodium orthovanadate and 0.1 M phenylmethylsulfonyl fluoride (PMSF)) and vortexed every 5 mins for 40 mins. The lysed cells were then centrifuged for 10 mins at 12 500 rpm. The protein, located in the supernatant, was removed and added to a fresh tube and quantified by Bramhall assay. A fresh sheet of filter paper was incubated in dH_2O for 20 mins followed by incubations in 95% ethanol, 100% ethanol, and 100% acetone with shaking (60 rpm) for 5 min each. The filter paper was left to dry for 10 min under the extraction hood. The standard curve was set up using 1 mg/ml of Bovine serum albumin (BSA) in 1x radioimmunoprecipitation assay (RIPA) buffer. Once the filter paper was dried, equal size circles for each standard, each sample, and controls (the buffers 1x RIPA without inhibitors to blank the standards and 1x RIPA with inhibitors to blank samples were used) were traced. Standards were spotted on the filter paper as follows: 1, 3, 6, 12, 16, & 20 µl followed by spotting 2 µl of each sample and each control. The filter paper was then dried under the extraction hood and incubated with 7.5% Trichloroacetic acid (TCA) for 45 min with shaking (60 rpm), followed by coomassie (1.3 g Coomassie blue powder, 50 ml acetic acid, and 250 ml methanol made up in dH_20) staining for 1 hr with shaking (60 rpm) and de-stained (10% acetic acid and 10% methanol made up to 250 ml with dH_2O) for 1 hr with shaking (60 rpm). The extraction hood was then used to dry the filter paper for 15 min and each circle was cut and placed in a test tube containing elution buffer (66 ml methanol, 33 ml dH_20, and 1 ml 25% ammonia) and incubated overnight in the dark with shaking (90 rpm). Followed by loading 160 µl of each standard, sample, and control in a 96- well plate. Absorbance was read at 595 nm.

3.5.3 SDS-PAGE and Transfer

Stacking (6%) and resolving (12%) polyacrylamide gels were prepared according to Table 1. Proteins were mixed with 6x protein loading buffer (300 mM tris pH 6.8, 600 mM Dithiothreitol (DTT), 12% SDS, 60% glycerol, and 0.6% Bromophenol Blue) (3:1 for 15 µg final protein concentration) vortexed, boiled for 5 min and vortex again. Once the SDS gel was set, 15 mg of each protein sample was then loaded into the SDS gel, and samples were resolved by Sodium Dodecyl Sulfate–Polyacrylamide Gel Electrophoresis (SDS-PAGE) for 65 min in SDS-running buffer (0.1 % SDS, 192mM glycine, 25 mM tris base, pH 8.8, stored at 4 °C before use) at 35 mA constant current.

Table 1: Polyacrylamide recipe for resolving and stacking gel

	12% resolving gel (ml)	6% Stacking gel (ml)
dH_20	3.3	3.265
29:1 Acrylamide/Bis-acrylamide	4.0	1
Tris (1.5 M pH 8.8 for resolving; 1 M pH 6.8 for stacking)	2.5	0.63
10% SDS	0.1	0.05
10% APS (Ammonium Persulphate)	0.1	0.05
TEMED (Tetramethylethylenediamine)	0.004	0.005

The SDS gel containing the resolved protein was then transferred to a nitrocellulose membrane by electroblotting at a constant current of 300 mA for 2 hrs at 4 °C in transfer buffer on ice in the fridge (192 mM glycine, 25 mM tris base, and 99,6 % methanol, pH 8.3).

3.5.4 Antibody Treatments and Detection

The nitrocellulose membranes were rinsed once with 1x TBS-T (20 mM tris base, 137 mM NaCl, and 0.1 % tween-20) for 5 min with shaking (90 rpm), followed by a 1 hr incubation at room temperature in blocking buffer (5% fat-free milk powder in 1x TBS-T) with gentle agitation (60 rpm). Membranes were then rinsed three times in 1x TBS-T for 5 min each and incubated with antibodies against β-actin (1/1000 β-actin, Santa Cruz Biotechnology) mouse monoclonal antibody in 5 % fat-free milk powder in 1x TBS-T) and γH2AX (1/1000 p-Histone H2A.X (Ser139) (Santa Cruz Biotechnology) mouse monoclonal antibody in 5 % BSA in 1x TBS-T), in the dark, overnight at 4 °C with gentle agitation (60 rpm). The membranes were then rinsed in 1x TBS-T five times for 5 min each with shaking (90 rpm) and incubated with secondary antibody (1/2000 m-IgGk BP- HRP (Santa Cruz Biotechnology) in 5 % fat-free milk powder in 1x TBS-T) in the dark, at room temperature with gentle agitation (60 rpm) for 1 hr. The membranes were then washed in 1x TBS- T five times for 5 min each with shaking (90 rpm). In a dark room, the membranes were exposed with SuperSignal West Pico PLUS Chemiluminescent Substrate (1:1 SuperSignal West Pico PLUS Luminol/Enhancer solution and SuperSignal West Pico PLUS stable peroxide solution) in the dark for 5 min. The membranes were then placed faced down and sealed with a clingfilm. The membranes were then exposed to x-ray film and the films were developed using a developer solution (6.4 M metol, 0,6 M sodium sulphite anhydrous, 80 mM hydroquinone, 45 mM sodium carbonate, and 34 mM potassium bromide) when bands became visible x-ray films were rinsed in water and fixed using a fixer solution (0.8 M sodium thiosulphate and 0.2 M sodium metasulphite made up in distilled water). The X-ray films were rinsed in water, set to dry, and scanned. Optical density was quantified using Image Studio Lite version 5.2.5 by Licor.

3.6 RT-PCR and qRT-PCR

To observe and quantify the level of expression of lncRNAs PANDA, ANRIL, and DDSR1 HEK293 and HT29 cells were treated with EC30 concentrations of NaCl for 4 hrs and 6 hrs. RNA was then extracted at 4 hrs NaCl only, 4 hrs NaCl with 5 min withdrawal, 6 hrs NaCl only, 6 hrs NaCl with 5 min withdrawal and untreated. RNA was then reverse transcribed to complementary DNA (cDNA), and reverse transcription polymerase chain reaction (RT-PCR) and quantitative reverse transcription PCR (qRT-PCR) were performed. Full methods are stated below.

3.6.1 RNA Extraction

RNA was extracted using TRI-reagent as per the product manual. Cells were lysed using 1 ml TRI reagent per 10 cm^2 cell culture dish and homogenised by pipetting the sample up and down several times to form a homogenous lysate. The homogenised sample was left to stand for 5 min at room temperature after which 0.2 ml of chloroform was added and the sample was vigorously shaken for 15 seconds and left to stand for 15 min at room temperature. The samples were then centrifuged at 12000 xG for 15 min at 4 °C. the samples were separated into 3 phases: the bottom of the tube contained the red organic phase with the proteins, the middle layer was the interphase containing DNA and at the top was the colourless aqueous phase containing RNA. The aqueous phase was carefully removed, added to a clean microcentrifuge tube and 0.5 ml of 2-propanol was added to each sample. The samples were then mixed and incubated at room temperature for 10 min. This was then centrifuged at 12000 xG at 4 °C for 10 min. The supernatant was removed, and the RNA pellet was washed with 1 ml of 75 % molecular grade ethanol by briefly vortexing and centrifuging the sample for 5 min at 7500 xG for 5 min. The RNA was dried for 10 min by air drying and dissolved in 50 µl autoclaved milli-q water at 55 °C for 15 min. RNA was quantified using the nanodrop and stored at -70 °C until further use. A typical DNase I (RNase-free) (NEB) was used to clean 10 µg of RNA from genomic DNA contamination. The RNA was treated with 1x DNaseI reaction buffer and 2 units of DNase (RNase-free) following the protocol manual. The reactions were incubated for 10 min at 37 °C. Followed by adding 1 µl of 0.5 M EDTA to each sample to chelate the Mg ions to inactivate the DNaseI with heat inactivation for 10 min at 75 °C.

3.6.2 cDNA Conversion

Following the Tetro cDNA synthesis kit (Celtic) protocol manual, reverse transcription was used to transcribe the RNA to cDNA. A reaction of 1 µg of RNA was converted to cDNA using 1 µl of random hexamer primers, 1 µl of 10 mM dNTP mix, 4 µl of 5x RT buffer, 1 µl of ribosafe RNase inhibitor, and 1 µl of tetro reverse transcriptase (200 u/µl). The reaction was made up to 20 µl using DEPC-treated water and incubated in a thermal cycler set up according to Table 2.

Table 2: cDNA synthesis thermocycler run conditions

Time	Temperature
10 min	25 °C
30 min	45 °C (or 48 °C: use of higher temperature may increase cDNA yield)
5 min	85 °C
∞	4 °C

3.6.3 RT-PCR

RT-PCR for lncRNAs PANDA, ANRIL, and DDSR1 expression was set up following the FastStart Master mix (Roche) protocol using the primers in Table 3.

Table 3: Forward and reverse Primers for lncRNAs PANDA, ANRIL & DDSR1 and housekeeping gene GAPDH with their respective melting temperatures and annealing temperatures

PRIMER	SEQUENCE	Tm	Ta
PANDA – FWD	5'- GAA GTC CTG ATG CAG ACC ATA A -3'	61.7 ℃	
PANDA – REV	5'- GAT AGC TGG AAA GCT GAG AGA G -3'	61.5 ℃	56,6 ℃
ANRIL – FWD	5'- CTA TCC GCC AAT CAG GAG GC -3'	63.8 ℃	
ANRIL – REV	5'- TCG TGG CAA ATA GTC CTA GTC C -3'	63.1 ℃	58.5 ℃
DDSR1 – FWD	5'- AAG AGT GGA AAA TTC ATC CCC A -3'	62 ℃	
DDSR1 – REV	5'- TGT CAT GTT TCA GAT ATT TTC CCC A -3'	62.8 ℃	57.4 ℃
GAPDH – FWD	5'- GTC AGT GGT GGA CCT GAC CT -3'	65 ℃	
GAPDH – REV	5'- AGG GGA GAT TCA GTG TGG TG -3'	63.1 ℃	59.1 ℃

RT-PCR reactions were set up for each sample using 25 ng cDNA and made up to a 1x mastermix final concentration and forward and reverse primers were added to a final concentration of 300 nM. RT-PCR was set up in a thermocycler set up according to Table 4.

Table 4: RT-PCR thermocycler conditions

Step	Temperature	Time	Cycles
Initial denaturation	95 °C	4 min	1
Denaturation	95 °C	30 sec	35
Annealing	PANDA: 56.6 °C ANRIL: 58.5 °C DDSR1: 57.4 °C GAPDH: 59.1 °C	30 sec	
Elongation	72 °C	45 sec	
Final extension	72 °C	7 min	1

Final RT-PCR products were resolved for 40 min at 90 V on a 2% agarose gel

3.6.4 qRT-PCR

qRT-PCR for lncRNAs PANDA, ANRIL and DDSR1 was then quantified using the SensiFast SYBR No-ROX kit (Celtic) as per the product manual. qRT-PCR reaction was set up for each sample using 100 ng cDNA and made up to a 1x mastermix final concentration and forward and reverse primers were added to a final concentration of 400 nM. qRT-PCR was completed using the Bio-Rad CFX96 Touch Real-Time PCR detection system and the qPCR thermocycling conditions were set up according to Table 5. Obtained qRT-PCR data was analysed using the Bio-Rad CFX maestro software.

Table 5: Bio-rad CFX96 thermocycler conditions

Step	Temperature	Time	Cycles
Initial denaturation	95 °C	2 min	1
Denaturation	95 °C	5 sec	35
Annealing	PANDA: 57.4 °C ANRIL: 59.2 °C DDSR1: 58.7 °C	10 sec	
Elongation	72 °C	20 sec	

3.7 Statistical Analysis

The students T-test was done on all data to determine if there was a significant difference between the means of the control (untreated) and the treatment groups. Significance was dictated according to Table 6.

Table 6: Statistical significance indicated by asterisks

Symbol	Meaning
ns	$P > 0.05$
*	$P \leq 0.05$
**	$P \leq 0.01$
***	$P \leq 0.001$
****	$P \leq 0.0001$

4 Results

4.1 Higher concentrations of NaCl are required to promote cytotoxicity in HT29 compared to HEK293 cells

Cell viability in the presence of NaCl was quantified by MTT assay and EC50 and EC30 values were determined in HEK293 and HT29 cell lines (Figure 3). Higher NaCl concentrations are seen to result in cell death in both HEK293 and HT29 cells as seen by lower absorbance values which correlate with a lower cell number. CurveExpert Basic software was used to analyse and construct a sigmoidal curve for each set of data (n=3).

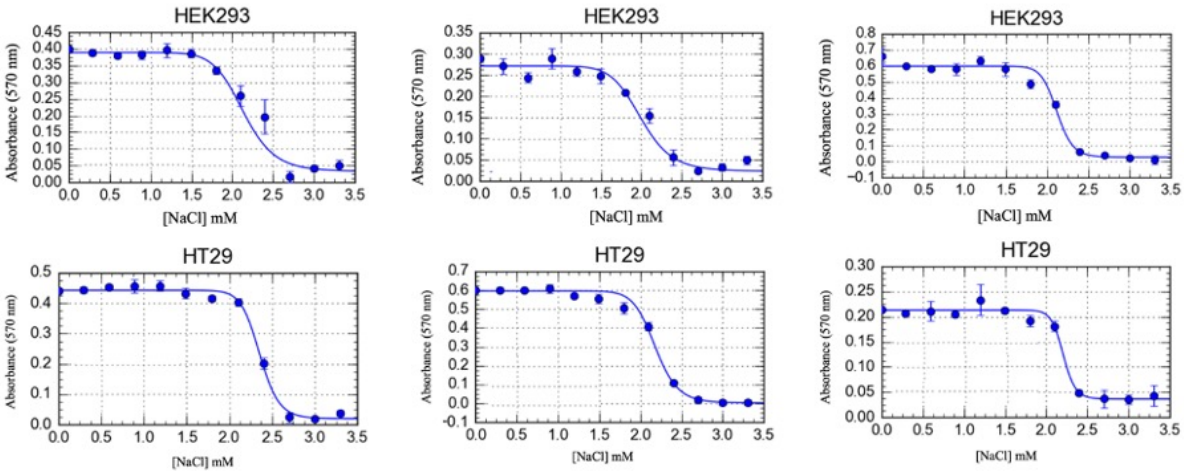

Figure 3: Cell viability assessed by MTT assay.

HEK293 and HT29 cells were treated with NaCl (0 mM -2000 mM) for 24 hrs and cell viability was measured by MTT assay (n=3). A) Data are shown as 3 separate experiments for HEK293 and HT29 cell lines. CurveExpert Basic was used to construct sigmoidal curves using DR-Hill.

The EC50 and EC30 values were determined for both HEK293 and HT29 cell lines (Table 7). The EC50 values were calculated to be 122.87 ± 20.32 mM and 180.26 ± 41.89 mM NaCl for HEK293 and HT29 cell lines respectively (n=3). The EC30 values were calculated to be 98.10 ± 18.35 mM and 149.61 ± 36.09 mM NaCl for HEK293 and HT29 cell lines respectively.The calculated EC50 values in HT29 were significantly higher compared to HEK293 (P-value = 0.05), suggesting that the HT29 cancer cells are less sensitive and more tolerant to high NaCl concentrations (Miermont et al., 2019).

Table 7: Calculated EC50 and EC30 values determined using DR-Hill equation (CurveExpert Basic) and standard deviations for HEK293 and HT 29 cell lines

	EC50 1	EC50 2	EC50 3	Average	Standard deviation
HEK293	132.03	99.59	137.00	122.87	20.32
HT29	228.41	152.16	160.22	180.26	41.89
	EC30 1	EC30 2	EC30 3	Average	Standard deviation
HEK293	110.09	76.98	107.24	98.10	18.35
HT29	190.57	122.49	135.76	149.61	36.09

]*

4.2 Mre11 translocated to the cytoplasm in the presence of NaCl and translocated to the nucleus upon withdrawal in HEK293 and HT29 cells

Nuclear translocation of Mre11 indicates that DNA damage response has been activated (Dmitrieva et al., 2003). This was measured using confocal microscopy of the protein Mre11 in response to NaCl treatment and NaCl withdrawal in HEK293 cells. Mre11 moves to the nucleus and nuclear periphery after NaCl withdrawal in HEK293 cells. In untreated cells, Mre11 can be seen mostly in the cytoplasm but can also be seen in the nucleus (Figure 4A and 4B). In response to NaCl treatment for 6 hrs (Figure 4A), Mre11 can be seen in the cytoplasm closer to the cell periphery and after 5 min NaCl withdrawal, Mre11 can be seen closer to the nuclear periphery and entering the nucleus. Similarly, in response to NaCl treatment for 24 hrs (Figure 4B) Mre11 can be seen in the mostly in the cytoplasm along the cell periphery and after 5 min NaCl withdrawal, Mre11 can be seen closer to the nuclear periphery and entering the nucleus.

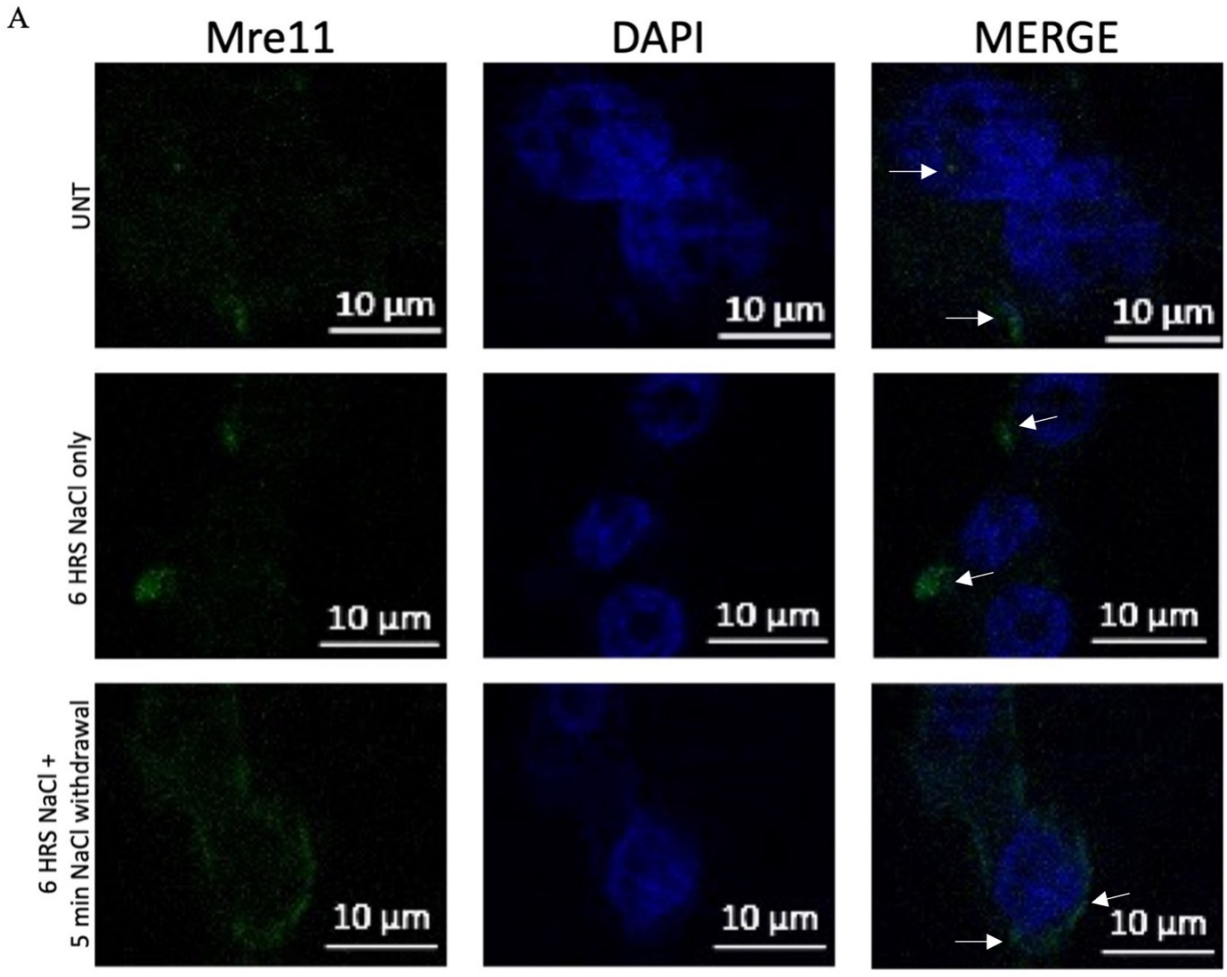

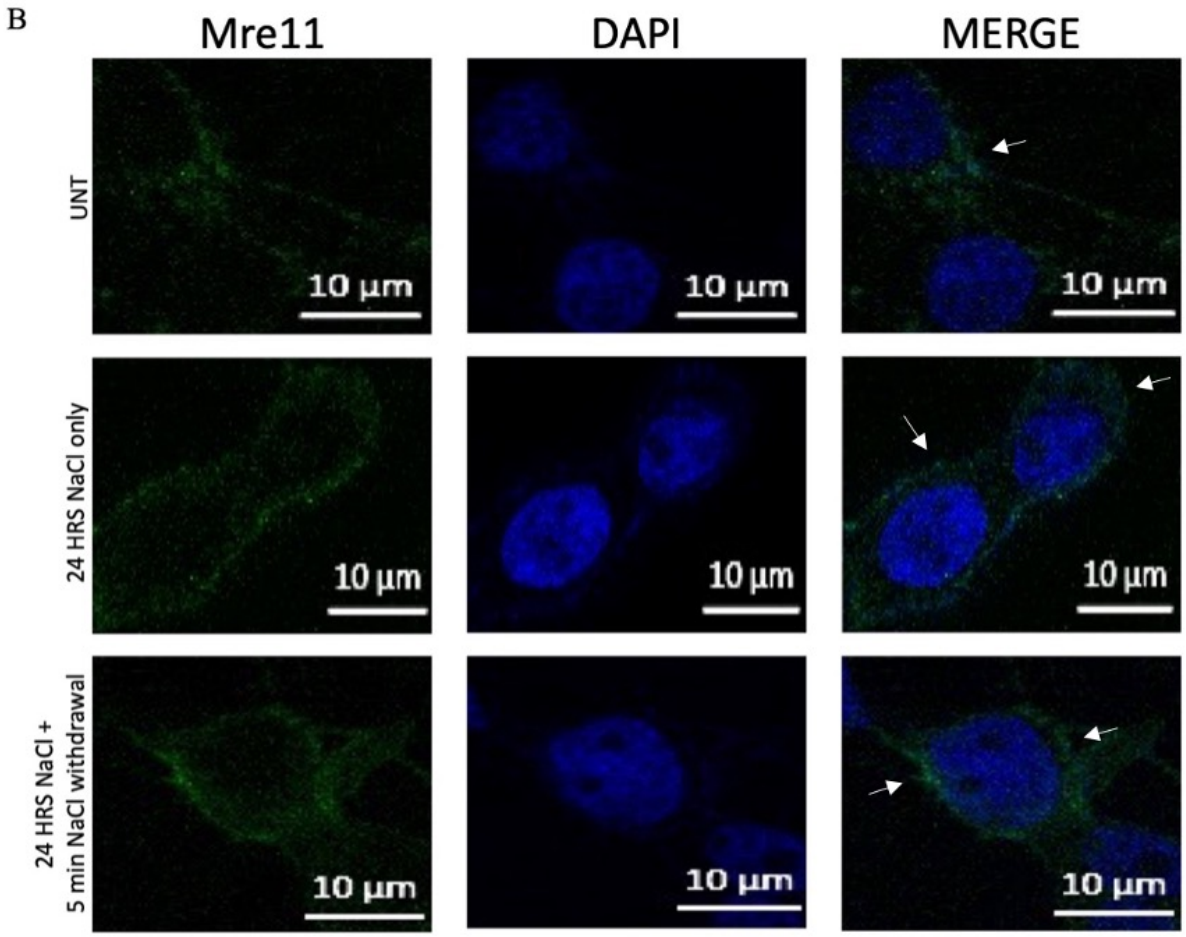

Figure 4: Mre11 localisation in HEK293 cells assessed by confocal microscopy.

Cells were treated with NaCl for 6 hrs, 6 hr NaCl followed by 5 min withdrawal (A) and NaCl for 24 hrs, 24 hr NaCl with 5 min withdrawal (B) and compared to respective untreated controls. Mre11 moves to the nucleus and nuclear periphery after NaCl withdrawal in HEK293 cells. In untreated cells, Mre11 localization is largely cytoplasmic and can be seen in the nucleus. During 6 hr and 24 hr NaCl, Mre11 is close to the cell periphery. After 5 min withdrawal for the 6 hr and 24 hr treatment groups, Mre11 moves closer to the nuclear periphery and enters the nucleus. Images were viewed and captured at 63x magnification.

In contrast, low expression of Mre11 was observed in HT29 cells (Figure 5A and 5B). In response to NaCl treatment for 6 hrs (Figure 5A), Mre11 was confined to the cytoplasm in untreated and 6 hrs NaCl treated cell. FITC was detected in the 6 hr NaCl and 5 min NaCl withdrawal, however, its expression was low. This could indicate that Mre11 is translocated to the nucleus or that the FITC signal detected is background fluorescence. Mre11 showed diffuse expression in 24 hr untreated cells. In response to 24 hrs NaCl, and 24 hr NaCl and 5 min NaCl withdrawal, Mre11 expression appeared to be localized in the cytoplasm (Figure 5B). This suggests that DDR signaling may be impaired after NaCl withdrawal in HT29 cells.

A

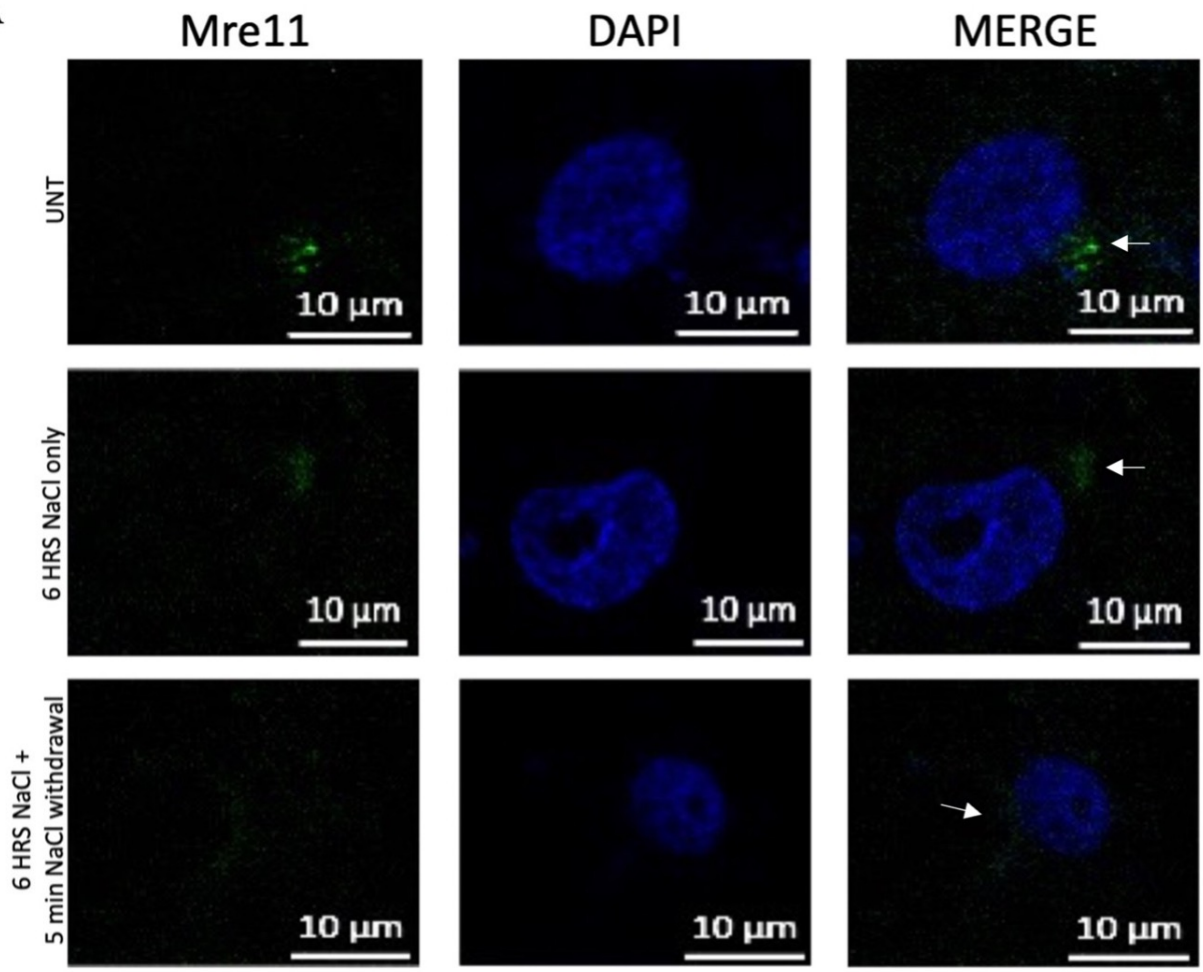
Mre11
DAPI
MERGE
UNT
6 HRS NaCl only
6 HRS NaCl +
5 min NaCl withdrawal
10 µm

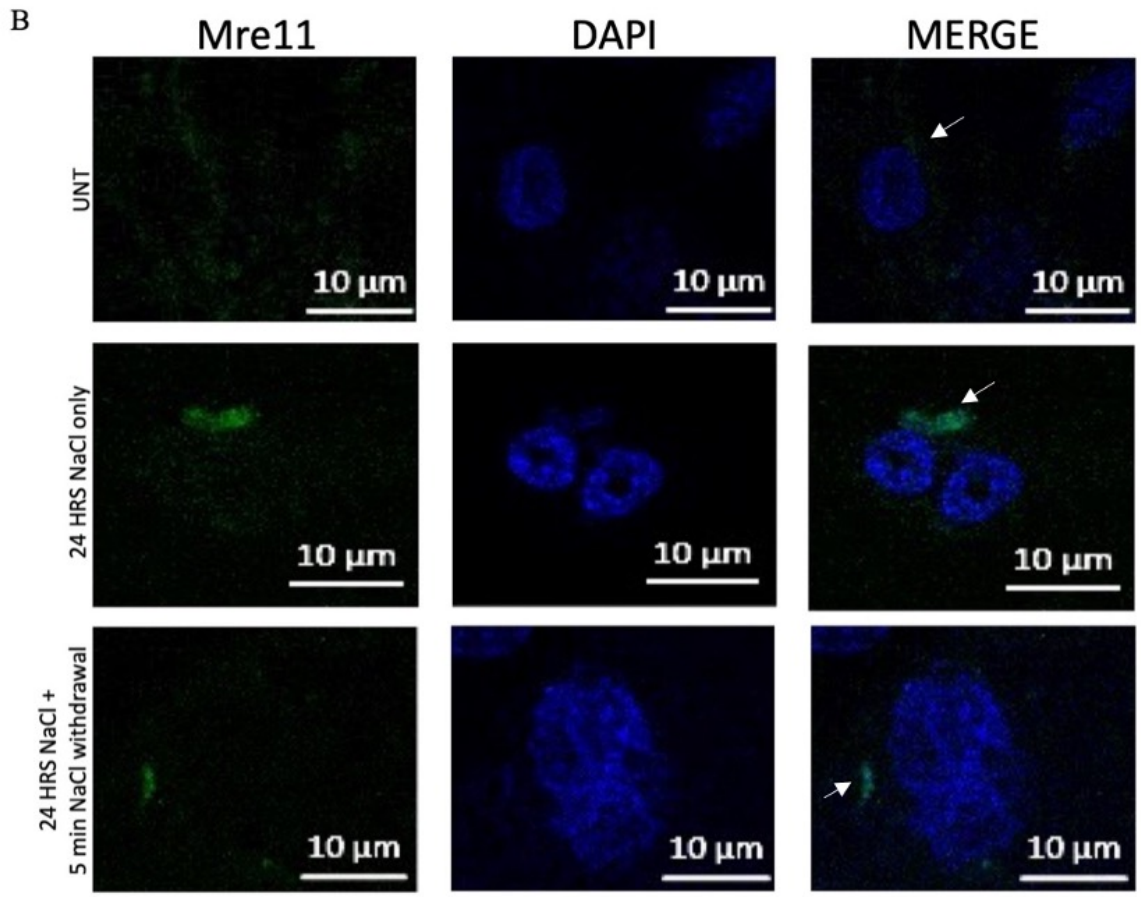

Figure 5: Mre11 localisation in HT29 cells assessed by confocal microscopy.

HT29 cells were treated with NaCl for 6 hrs, 6 hr NaCl followed by 5 min withdrawal (A) and NaCl for 24 hrs, 24 hr NaCl with 5 min withdrawal (B) and compared to respective untreated controls. Mre11 was confined to the cytoplasm in untreated and 6 hr NaCl treated cells. Low expression of Mre11 was observed after 5 min NaCl withdrawal. However, FITC signal was detected in the nucleus. This could indicate Mre11 nuclear translocation or background fluorescence. Diffuse expression of Mre11 was detected in 24 hr untreated cells. Mre11 appeared to be localized in the cytoplasm in the 24 hr NaCl and 24 hr NaCl and 5 min withdrawal treatment groups suggesting an impairment in DNA damage response signaling after NaCl withdrawal in HT29 cells. Images were viewed and captured at 63x magnification.

This data may suggest that DDR may be activated in HEK293 cells as seen by Mre11 nuclear translocation. However, it is unclear if HT29s are repairing their DNA with a high efficiency due to low diffuse FITC signal detected throughout all cell treatment groups. Additionally, the cytoplasmic localization of Mre11 in the 24 hr NaCl and 24 hrs NaCl and 5 min NaCl withdrawal treatment groups seemed to co-localize with DAPI. This suggests that nuclear deformation may lead to spillage of DNA into the cytoplasm in a hypertonic environment (Finan and Guilak, 2010).

4.3 γH2AX levels are not significantly altered after NaCl treatment in HEK293 and HT29 cell lines

γH2AX expression is an early DSB marker that is crucial for DNA repair (Podhorecka et al., 2010). Western blot analysis for γH2AX expression was used to quantify DSB formation in NaCl treated and untreated HEK293 and HT29 cell lines. γH2AX expression was normalised against b-actin. There was no significant change in γH2AX expression in both HEK293 and HT29 cell lines (P- values > 0.05) (Figure 6). Whilst there was no significant change, there did appear to be a slight increase in γH2AX expression in HEK293. This may suggest an increase in DNA repair signalling, but it is not significant enough to confirm that DNA DSB formation was increased in response to NaCl treatment after 4 hrs and 6 hrs. There was a slight, albeit insignificant, reduction in γH2AX expression in HT29 (n=3). This suggests one of two things, firstly that there is no increase in DNA DSB formation or that DSBs are rapidly repaired and γH2AX is dephosphorylated by WIP1. Low expression of γH2AX may be indicative of dephosphorylation of γH2AX that subsequently suppresses the activation of downstream DDR-activated proteins and halts DNA repair pathways (Macůrek et al., 2010).

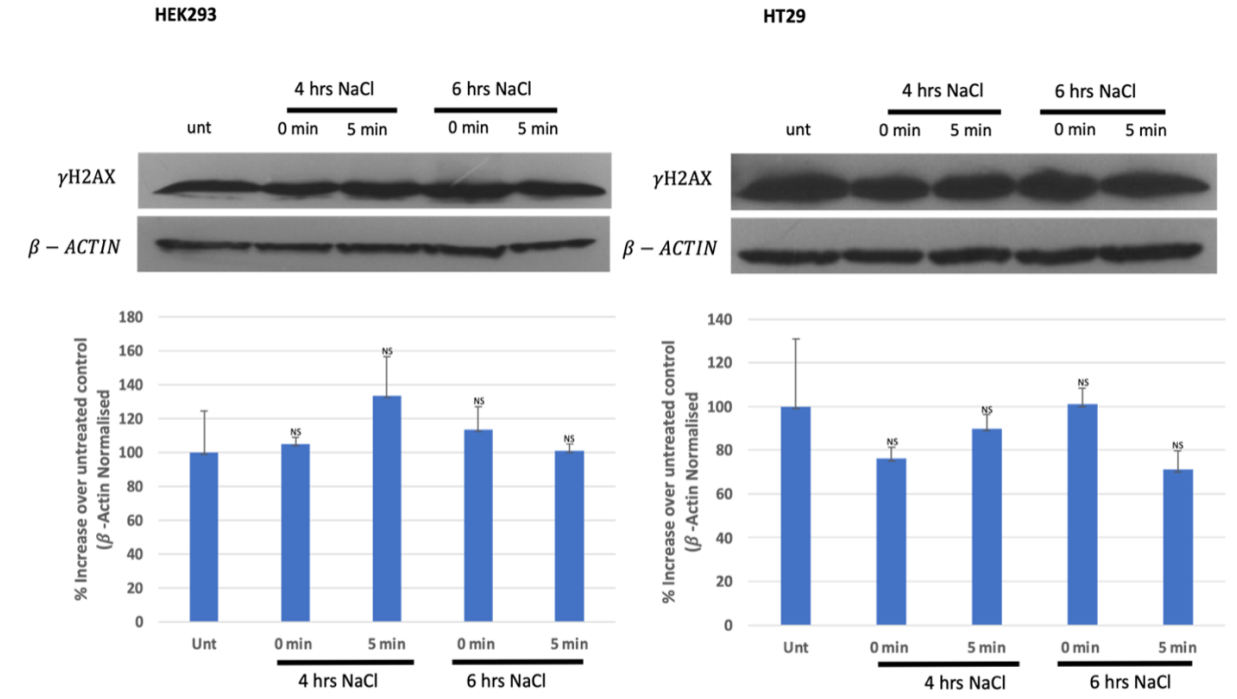

Figure 6: DNA damage repair observed by γH2AX expression by western blot analysis.

HEK293 and HT29 cells were treated with NaCl for 4 hrs and 6 hrs and harvested at 0 min and 5 min NaCl withdrawal. γH2AX expression was normalized against b-Actin. There is no significant change in γH2AX expression in both HEK293 and HT29 cells (P-Value > 0.05). However, γH2AX expression is slightly reduced in HT29 cells, whereas in HEK293 cells γH2AX expression is slightly elevated (n=3) biological replicates.

4.4 4.4. lncRNA expression in response to NaCl treatment

The dysregulation of lncRNAs modulating DDR signalling pathways, such as the ATM, ATR and p53 pathways, has become a point of interest in cancer research. The lncRNAs PANDA and ANRIL have roles in DDR by regulating cell cycle progression, and DDSR1 has a role in DNA repair by promoting HR (Kong et al., 2018; Puvvula, 2019; Sharma et al., 2015). RT-PCR analysis of lncRNAs PANDA, ANRIL and DDSR1 for HEK293 (Figure 7A) and HT29 (Figure 7B) was conducted to assess primer annealing temperatures and to ensure that there was no non-specific binding. qRT-PCR products are sensitive to non-specific binding of unrelated targets that occur frequently and are unrelated to the efficiency of obtained Cq values. The 2-step RT-PCR assists in controlling the annealing temperature in which the primers anneal to the cDNA strand and itself (Ruiz-Villalba et al., 2017). RT-PCR data for lncRNAs PANDA, ANRIL, and DDSR1 in HEK293 (Figure 7A) and HT29 (Figure 7B) cell lines showed a single band for all NaCl treatment (4 hr and 6 hr NaCl treatment groups) and NaCl withdrawal groups (4 hrs NaCl and 5 min NaCl withdrawal and 6 hrs NaCl and 5 min NaCl withdrawal) as well as the untreated control for each cell line. A faint band below the 50 bp MW was present in all three lncRNAs for all untreated, NaCl treatment and NaCl withdrawal groups in both HEK293 and HT29 cell lines are indicative of the primers bind to each other.

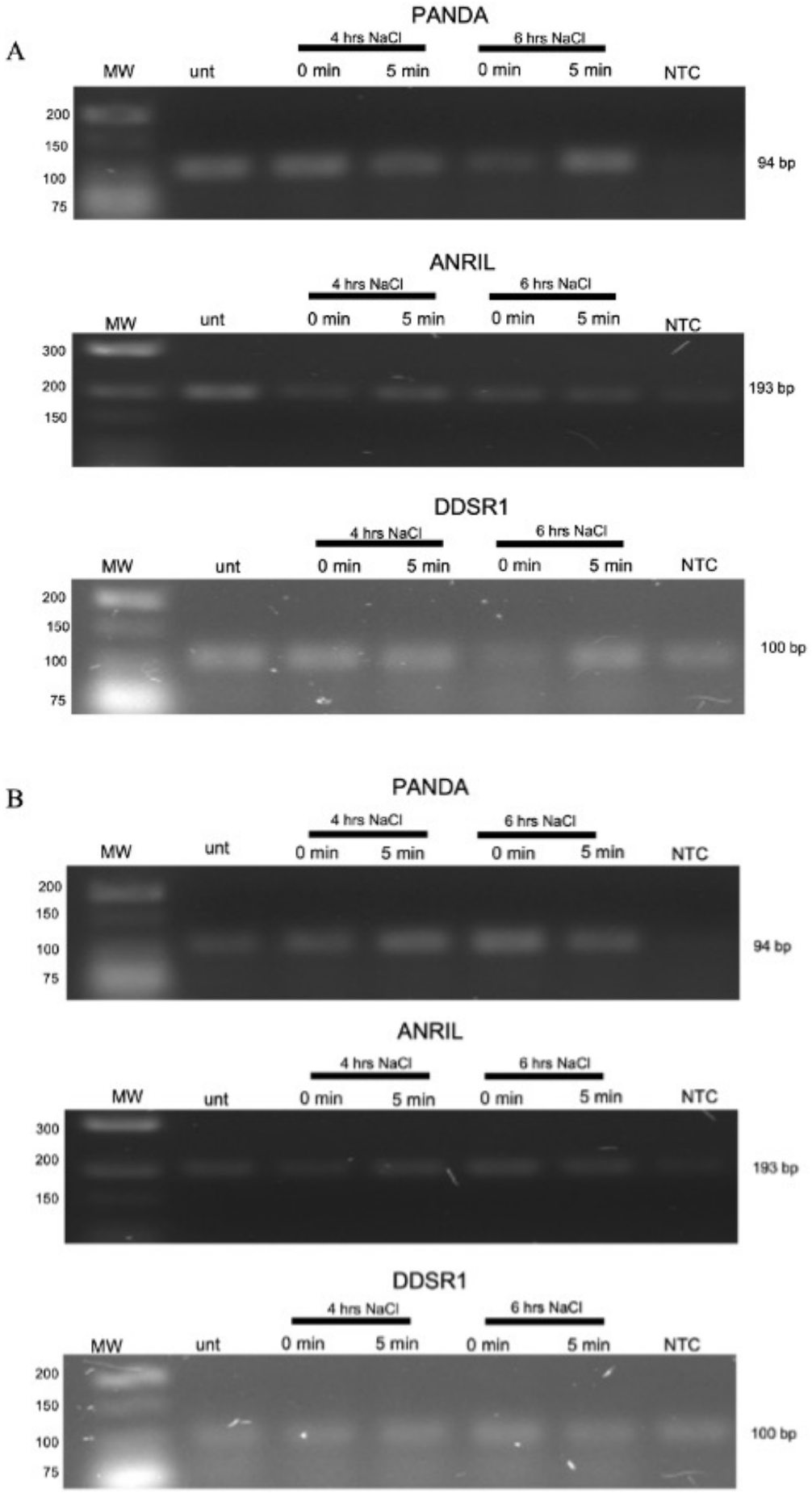
A
PANDA
4 hrs NaCl
6 hrs NaCl
MW
unt
0 min
5 min
0 min
5 min
NTC
200
150
100
75
94 bp
ANRIL
4 hrs NaCl
6 hrs NaCl
MW
unt
0 min
5 min
0 min
5 min
NTC
300
200
150
193 bp
DDSR1
4 hrs NaCl
6 hrs NaCl
MW
unt
0 min
5 min
0 min
5 min
NTC
200
150
100
75
100 bp
B
PANDA
4 hrs NaCl
6 hrs NaCl
MW
unt
0 min
5 min
0 min
5 min
NTC
200
150
100
75
94 bp
ANRIL
4 hrs NaCl
6 hrs NaCl
MW
unt
0 min
5 min
0 min
5 min
NTC
300
200
150
193 bp
DDSR1
4 hrs NaCl
6 hrs NaCl
MW
unt
0 min
5 min
0 min
5 min
NTC
200
150
100
75
100 bp

Figure 7: LncRNA expression analysis for PANDA, ANRIL and DDSR1 analysed by RT-PCR.

RT-PCR for lncRNAs PANDA, ANRIL and DDSR1 were analyzed by electrophoresis and run on a 2% agarose gel in HEK293 (A) and HT29 (B) cell lines. RT-PCR showed single bands for all treatment groups (4 hr NaCl, 4 hrs NaCl and 5 min NaCl withdrawal, 6 hr NaCl and 6 hrs NaCl and 5 min NaCl withdrawal) and untreated control groups for both HEK293 and HT29 cell lines.

LncRNA expression for PANDA, ANRIL and DDSR1 was quantified by qRT-PCR in HEK293 and HT29 (Figure 8A and 8B) cell lines. LncRNAs expression for PANDA, ANRIL, and DDSR1 in HEK293 cells (Figure 8A) was significantly reduced for 4 hr and 6 hr NaCl treatment groups and 4 hr NaCl and 5 min NaCl withdrawal groups and 6 hr NaCl and 5 min NaCl withdrawal groups compared to the untreated control group. In contrast, in the HT29 cell line (Figure 8B) lncRNA expression analysis for PANDA and ANRIL show significant increased expression at 4 hrs NaCl, and 6 hrs NaCl and 5 min NaCl withdrawal. Whereas, expression for both PANDA and ANRIL was reduced at 4 hrs NaCl and 5 min NaCl withdrawal and 6 hrs NaCl. LncRNA DDSR1 expression was significantly increased at 6 hrs NaCl only and DDSR1 expression was reduced at 4 hrs NaCl and 6 hrs NaCl and 5 min NaCl withdrawal, while the 4 hrs NaCl treatment showed expression levels similar to the untreated control group.

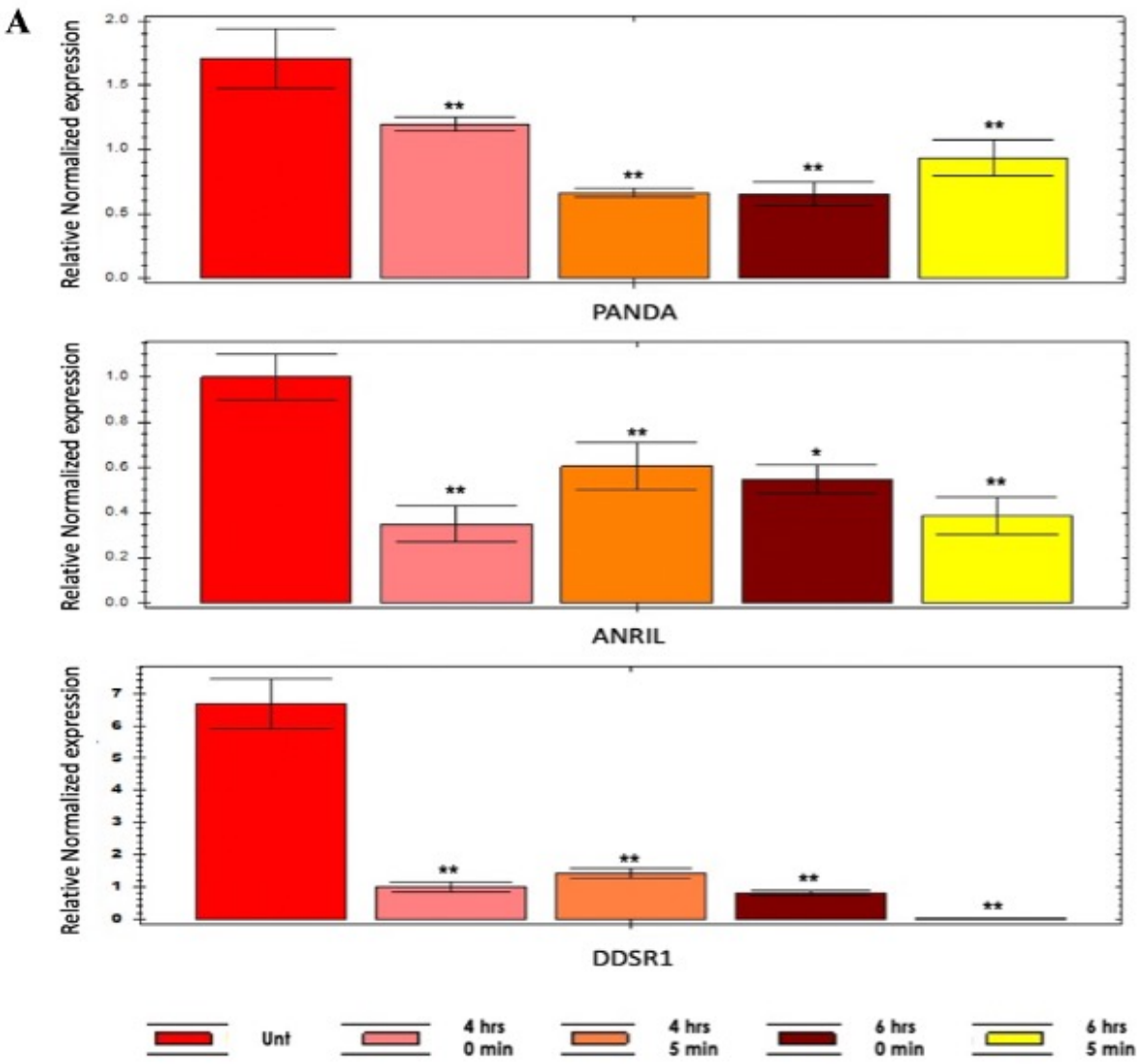
A
Relative Normalized expression
2.0
1.5
1.0
0.5
0.0
**
**
**
**
PANDA
Relative Normalized expression
1.0
0.8
0.6
0.4
0.2
0.0
**
**
*
**
ANRIL
Relative Normalized expression
7
6
5
4
3
2
1
0
**
**
**
**
DDSR1
Unt
4 hrs 0 min
4 hrs 5 min
6 hrs 0 min
6 hrs 5 min

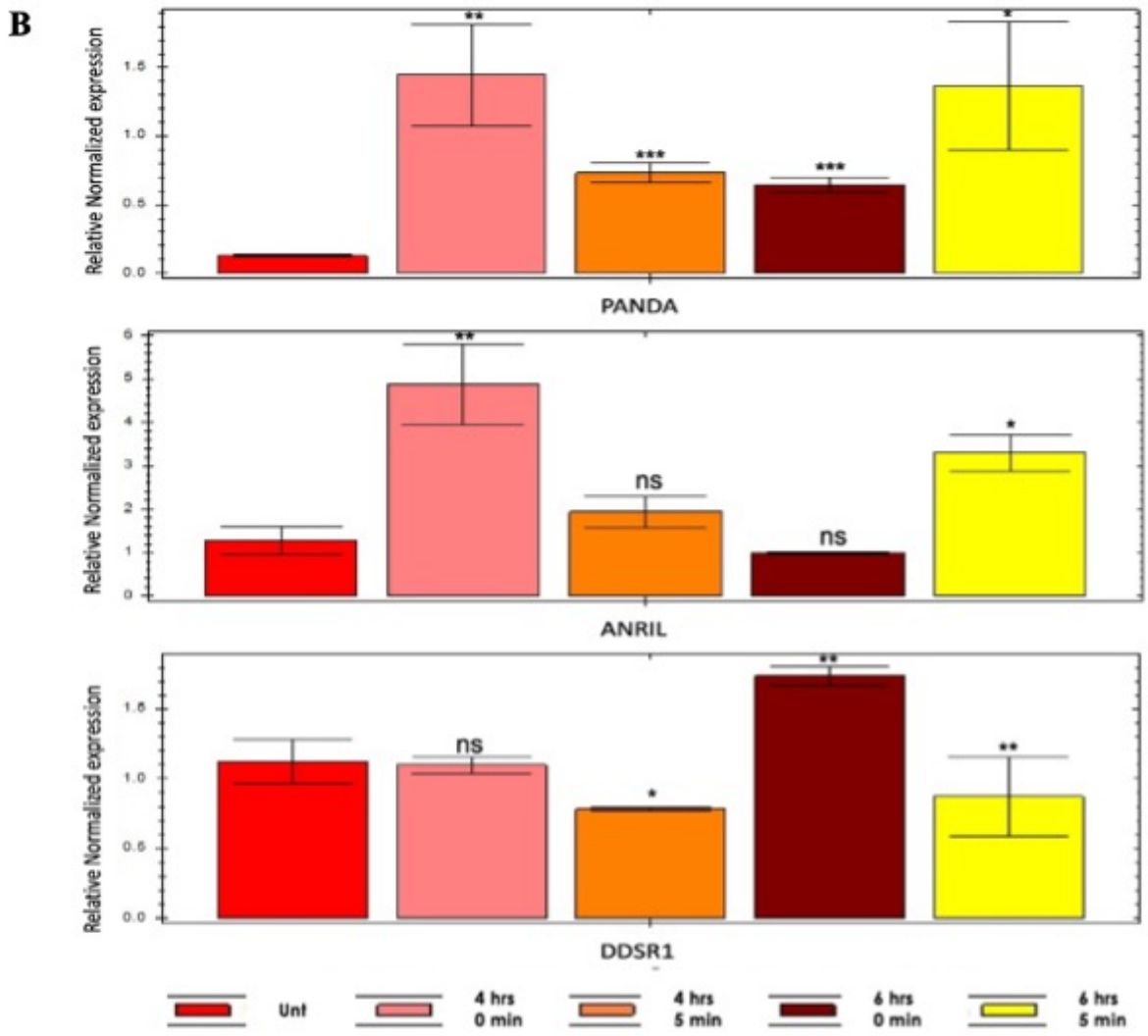

Figure 8: DNA damage associated lncRNA expression of lncRNAs PANDA, ANRIL, and DDSR1 in response to NaCl treatment and withdrawal by qRT-PCR.

Quantification of lncRNA expression by qRT-PCR in HEK293(A) and HT29 (B) cell lines. qRT-PCR analysis of lncRNA expression in HEK293 cells shows reduced lncRNA expression for NaCl treatment (4 hrs NaCl and 6 hrs NaCl treatments) and NaCl withdrawals (4 hrs NaCl and 5 min withdrawal and 6 hrs NaCl and 5 min withdrawal) groups for lncRNAs PANDA, ANRIL and DDSR1. While qRT-PCR analysis for lncRNA PANDA shows a significant increase in expression for all treatments; 4 hrs and 6 hrs NaCl+ 0 min NaCl withdrawal and 4 hrs and 6 hrs NaCl + 5 min NaCl withdrawal. LncRNA ANRIL shows a significant increase in expression at 4 hrs NaCl and 6 hrs NaCl and 5 min NaCl withdrawal. And DDSR showed a significant increase in expression at 6 hrs NaCl treatment only (n=1). Error bars were calculated from three technical replicates.

Overall, lncRNA expression was reduced in response to NaCl in the HEK293 cell line. This may indicate that the HEK293 cells respond to NaCl by reducing transcription in general (Burg et al., 2007), as expected. However, in the HT29 cell line, we see a significant upregulation and no significant down regulation of lncRNA expression. This indicates that these cells may

still be growing and proliferating in the hypertonic medium, and that these lncRNAs may overcome the DNA damage response and promote consistent cell cycle progression, even in the absence of DNA repair.

5 Discussion

In this study, we aimed to determine if DNA damage associated lncRNAs have altered regulation in response to DSBs induced by hypertonic media. When HEK293 and HT29 cell lines were exposed to high NaCl concentrations for 24 hrs, we found that the HT29 cancer cell line was more tolerant to high NaCl conditions. In HT29 the calculated EC50 180.26 ± 41.89 mM was significantly higher than the HEK293 cells EC50 122.87 ± 20.23 mM indicating that HT29 are less sensitive to increased NaCl conditions and adapt better to hypertonic environments. Previous studies indicate that cancer cells may have a higher salt microenvironment compared to normal cells and suggest that the NFAT5 transcription factor is induced in high salt environments and promotes inflammation and pro-angiogenic responses in tumors (Amara and Tiriveedhi, 2017; Leslie et al., 2019), that contributes to their survival and growth (Amara et al., 2016). In addition, our data suggest that the more tolerant HT29 cells are better suited to hypertonic environments as they may already have mechanisms in place to cope with high salt environments that also contribute to cancer proliferation and metastasis.

We found that DNA damage was not significantly induced in either of the two cell lines in the hypertonic medium as indicated by no significant change in γH2AX levels. However, nuclear translocation of Mre11 during the 5 min NaCl withdrawal stage suggested that DDR signalling was activated in both cell lines after both 6 hr and 24 hr NaCl treatment. Recent studies provide insight into the osmoregulation of cancer cells and suggest that cancer cells are less sensitive to high NaCl environments (Miermont et al., 2019). This and the Mre11 data obtained in this study would suggest that in hypertonic situations cancer cells have mechanisms in place to accommodate this increase in NaCl, such as coping with the volume change, and most likely have alternative pathways activated, thus allowing HT29 cells to continue repairing damaged DNA while still in an osmoprotective state due to osmotic stress (Burg et al., 2007; Casali et al., 2018).

LncRNA expression was downregulated in response to NaCl in HEK293 cells. Reduced expression of these lncRNAs may be the result of reduced transcription in hypertonic media

(Burg et al., 2007). To better observe the pattern of lncRNA expression following DNA damage, it may be useful to include more time points after exposure to a damage-inducing agent. Contrary to HEK293, lncRNA expression in HT29 cells was significantly higher in all NaCl treatment groups. PANDA and ANRIL levels were significantly elevated in the 4 hr treatment group, but expression levels were reduced in the 5 min withdrawal compared to the 4 hr NaCl only. This may suggest that the cell cycle may be transiently arrested to allow for DNA repair since ANRIL and PANDA expression are required for continued cell cycle progression (Kong et al., 2018; Puvvula, 2019). It would be useful to confirm this by performing cell cycle analysis with flow cytometry. ANRIL and PANDA expression was also significantly higher in the 6 hr with 5 min withdrawal treatment group. Considering that both these lncRNAs act as inhibitors of CDKNs, they are associated with continued cell cycle progression, which may occur in the absence of DNA repair in the cancer cell line. Overall, data for these two lncRNAs suggest that HT29 cells are able to cope better with NaCl and continue cell cycle progression in the first 4 hrs of NaCl treatment, but lower expression at the 6 hr NaCl compared to the 4 hr NaCl time point suggests that cell cycle progression may be reduced after 6 hr NaCl incubation. Elevated levels of ANRIL and PANDA in the 6 hr NaCl with 5 min with withdrawal group as compared to the 6 hr treatment group suggest that these cells may continue cell cycle progression immediately following NaCl withdrawal. DDSR1 levels were significantly elevated in the 6 hr treatment group. Since DDSR1 is involved in DNA repair by homologous recombination (Sharma et al., 2015), its upregulation suggests that the cancer cell line is still undergoing mitosis and utilizing this pathway for DNA repair in the presence of NaCl. DDSR1 levels were stable in all other treatment groups. Whilst this dataset provides reasonable grounds to further investigate lncRNA ANRIL and PANDA at the functional level, it would be useful to conduct more biological replicates.

6 Limitations and Future Directions

To ensure that the outcome of each data set was attributed to increased NaCl conditions, three biological replicates and three technical replicates for each biological replicate were completed for MTT assay, three biological replicates were completed for western blot analysis, one biological replicate was completed for confocal microscopy and RT-PCR and two biological replicates and three technical replicates for each biological replicate was completed for qRT-PCR. Data obtained from MTT assays showed a significantly higher NaCl tolerance in HT29 cells compared to the HEK293 cells. While western blot data had a high statistical significance

between the biological replicates, suggesting that the data obtained may be due to random biological variation rather than increased NaCl concentrations. Whilst two biological replicates were performed for qRT-PCR, insufficient data was obtained from the second biological replicate due to time constraints. As only one biological replicate showed complete results this was not sufficient to conduct statistical analysis with biological replicates. At least two more complete biological replicates are required to make a reliable conclusion.

This study aimed to observe the altered expression levels of DNA damage associated lncRNAs PANDA, ANRIL, and DDSR1 in response to DNA damage induced by increased NaCl concentrations. There are multiple mechanisms in which DNA is repaired depending on the type of DNA damage. Cancer cells are known to bypass DDR pathways and have multiple dysfunctions in these DDR pathways. Recent discoveries have shown that some lncRNAs are able to sense and regulate gene activity in response to DNA damage (Su et al., 2018). LncRNA expression has been dysregulated in many cancers and because lncRNAs circulate in many body fluids they can be used as potential novel biomarkers to diagnose cancer (Tehrani et al., 2018). Future studies to identify and characterise the lncRNAs that function in early in sensing and signalling for DDR may contribute to better and earlier diagnosis and prognosis of different cancer types.

7 Conclusion

In conclusion, we found that the HT29 cancer cells were more tolerant to NaCl, compared to the non-cancer HEK293 cell line. This suggests that the HT29 cells may have additional osmoprotective mechanisms in place to help them cope in a hypertonic microenvironment. In HEK293 cells Mre11is translocated to the cytoplasm under high NaCl conditions and is translocated back to the nucleus when NaCl is removed, but Mre11 is present in both the nucleus and the cytoplasm in HT29 cells. This may suggest that the HT29 cells may still be able to sense DSBs even in the presence of NaCl. γH2AX showed no significant change in expression, however, γH2AX expression was slightly reduced in the HT29s, which may be attributed to dephosphorylation of γH2AX during DNA repair. LncRNAs PANDA, ANRIL, and PANDA expression is reduced in HEK293 cells but is elevated in HT29 cells suggesting that HT29 cells may still be undergoing cell cycle arrest, DNA repair, and proliferation in hypertonic environments.

8 References

Aleksandrov, R., Hristova, R., Stoynov, S., Gospodinov, A., 2020. The Chromatin Response to Double-Strand DNA Breaks and Their Repair. Cells 9, 1853. https://doi.org/10.3390/cells9081853

Amara, S., Alotaibi, D., Tiriveedhi, V., 2016. NFAT5/STAT3 interaction mediates synergism of high salt with IL-17 towards induction of VEGF-A expression in breast cancer cells. Oncology Letters 12, 933–943. https://doi.org/10.3892/ol.2016.4713

Amara, S., Tiriveedhi, V., 2017. Inflammatory role of high salt level in tumor microenvironment (Review). International Journal of Oncology 50, 1477–1481. https://doi.org/10.3892/ijo.2017.3936

Argyropoulos, C., Rondon-Berrios, H., Raj, D.S., Malhotra, D., Agaba, E.I., Rohrscheib, M., Khitan, Z., Murata, G.H., Shapiro, J.I., Tzamaloukas, A.H., 2016. Hypertonicity: Pathophysiologic Concept and Experimental Studies. Cureus Journal of Medical Science 8, e596. https://doi.org/10.7759/cureus.596

Balas, M.M., Johnson, A.M., 2018. Exploring the mechanisms behind long noncoding RNAs and cancer. Non-coding RNA Research 3, 108–117. https://doi.org/10.1016/J.NCRNA.2018.03.001

Batenburg, N.L., Walker, J.R., Coulombe, Y., Sherker, A., Masson, J.-Y., Zhu, X.-D., 2019. CSB interacts with BRCA1 in late S/G2 to promote MRN-and CtIP-mediated DNA end resection. Nucleic Acids Research 47, 10678–10692. https://doi.org/10.1093/nar/gkz784

Bernstein, C., Prasad, A.R., Nfonsam, V., Harris Bernstein, 2013. DNA Damage, DNA Repair and Cancer. New Research Directions in DNA Repair. https://doi.org/10.5772/53919

Bian, L., Meng, Y., Zhang, M., Li, D., 2019. MRE11-RAD50-NBS1 complex alterations and DNA damage response: implications for cancer treatment. Molecular Cancer 18, 169. https://doi.org/10.1186/s12943-019-1100-5

Burg, M.B., Ferraris, J.D., Dmitrieva, N.I., 2007. Cellular response to hyperosmotic stresses. Physiological Reviews 87, 1441–1474. https://doi.org/10.1152/PHYSREV.00056.2006/ASSET/IMAGES/LARGE/Z9J0040724510003.JPEG

Burkewitz, K., Choe, K., Strange, K., 2011. Hypertonic stress induces rapid and widespread protein damage in C. elegans. American Journal of Physiology - Cell Physiology 301, C566. https://doi.org/10.1152/AJPCELL.00030.2011

Calin, G.A., Liu, C., Ferracin, M., Hyslop, T., Spizzo, R., Sevignani, C., Fabbri, M., Cimmino, A., Lee, E.J., Wojcik, S.E., Shimizu, M., Tili, E., Rossi, S., Taccioli, C., Pichiorri, F., Liu, X., Zupo, S., Herlea, V., Gramantieri, L., Lanza, G., Alder, H., Rassenti, L., Volinia, S., Schmittgen, T.D., Kipps, T.J., Negrini, M., Croce, C.M., 2007. Ultraconserved regions encoding ncRNAs are altered in human leukemias and carcinomas. Cancer Cell 12, 215–229. https://doi.org/10.1016/j.ccr.2007.07.027

Casali, C.I., Erjavec, L.C., Fernández-Tome, M. del C., 2018. Sequential and synchronized hypertonicity-induced activation of Rel-family transcription factors is required for osmoprotection in renal cells. Heliyon 4, e01072. https://doi.org/10.1016/j.heliyon.2018.e01072

Chang, H.H.Y., Pannunzio, N.R., Adachi, N., Lieber, M.R., 2017. Non-homologous DNA end joining and alternative pathways to double-strand break repair. Nature Reviews Molecular Cell Biology 18, 495. https://doi.org/10.1038/NRM.2017.48

Chatterjee, N., Walker, G.C., 2017. Mechanisms of DNA damage, repair, and mutagenesis. Environmental and Molecular Mutagenesis 58, 235–263. https://doi.org/10.1002/em.22087

Chen, H., Lisby, M., Symington, L.S., 2013. RPA Coordinates DNA End Resection and Prevents Formation of DNA Hairpins. Molecular Cell 50, 589–600. https://doi.org/10.1016/J.MOLCEL.2013.04.032

Congrains, A., Kamide, K., Ohishi, M., Rakugi, H., 2013. ANRIL: Molecular Mechanisms and Implications in Human Health. International Journal of Molecular Sciences 14, 1278–1292. https://doi.org/10.3390/ijms14011278

Das, S., Reddy, M.A., Natarajan, R., 2020. Role of epigenetic mechanisms regulated by enhancers and lncRNAs in cardiovascular disease. Current Opinion in Cardiology 35, 234. https://doi.org/10.1097/HCO.0000000000000728

Davis, A.J., Chen, D.J., 2013. DNA double strand break repair via non-homologous end-joining. Translational Cancer Research 2, 130–143. https://doi.org/10.3978/j.issn.2218-676X.2013.04.02

Dmitrieva, N.I., Bulavin, D. v, Burg, M.B., 2003. High NaCl causes Mre11 to leave the nucleus, disrupting DNA damage signaling and repair. American Journal of Physiology-Renal Physiology 285, F266–F274. https://doi.org/10.1152/ajprenal.00060.2003

Dmitrieva, N.I., Burg, M.B., 2008. Analysis of DNA breaks, DNA damage response, and apoptosis produced by high NaCl. American Journal of Physiology-Renal Physiology 295, F1678–F1688. https://doi.org/10.1152/ajprenal.90424.2008

Dmitrieva, N.I., Cui, K., Kitchaev, D.A., Zhao, K., Burg, M.B., 2011. DNA double-strand breaks induced by high NaCl occur predominantly in gene deserts. Proceedings of the National Academy of Sciences 108, 20796–20801. https://doi.org/10.1073/pnas.1114677108

Duch, A., de Nadal, E., Posas, F., 2012. The p38 and Hog1 SAPKs control cell cycle progression in response to environmental stresses. FEBS Letters 586, 2925–2931. https://doi.org/10.1016/j.febslet.2012.07.034

Dudáš, A., Chovanec, M., 2004. DNA double-strand break repair by homologous recombination. Mutation Research/Reviews in Mutation Research 566, 131–167. https://doi.org/10.1016/J.MRREV.2003.07.001

Eren, M.K., Kartal, N.B., Pilevneli, H., 2021. Oncogenic WIP1 phosphatase attenuates the DNA damage response and sensitizes p53 mutant Jurkat cells to apoptosis. Oncology Letters 21, 1–10. https://doi.org/10.3892/OL.2021.12740/HTML

Fan, Y.L., Zhao, H.C., Feng, X.Q., 2021. Hypertonic pressure affects the pluripotency and self-renewal of mouse embryonic stem cells. Stem Cell Research 56, 1873–5061. https://doi.org/10.1016/J.SCR.2021.102537

Fang, Y., Fullwood, M.J., 2016. Roles, Functions, and Mechanisms of Long Non-coding RNAs in Cancer. Genomics, Proteomics & Bioinformatics 14, 42–54. https://doi.org/10.1016/J.GPB.2015.09.006

Ferrè, F., Colantoni, A., Helmer-Citterich, M., 2016. Revealing protein–lncRNA interaction. Briefings in Bioinformatics 17, 106–116. https://doi.org/10.1093/bib/bbv031

Finan, J.D., Guilak, F., 2010. The effects of osmotic stress on the structure and function of the cell nucleus. Journal Cellular Biochemisrty 109, 460. https://doi.org/10.1002/JCB.22437

Giglia-Mari, G., Zotter, A., Vermeulen, W., 2011. DNA Damage Response. Cold Spring Harbor Perspectives in Biology 3. https://doi.org/10.1101/cshperspect.a000745

Gupta, S.C., Tripathi, Y.N., 2017. Potential of long non-coding RNAs in cancer patients: From biomarkers to therapeutic targets. International Journal of Cancer. https://doi.org/10.1002/ijc.30546

Habraken, Y., Piette, J., 2006. NF-κB activation by double-strand breaks. Biochemical Pharmacology 72, 1132–1141. https://doi.org/10.1016/J.BCP.2006.07.015

Hadjicharalambous, M.R., Lindsay, M.A., 2019. Long non-coding RNAs and the innate immune response. Noncoding RNA 5. https://doi.org/10.3390/NCRNA5020034

Han, J., Huang, J., 2020. DNA double-strand break repair pathway choice: the fork in the road. Genome Instability & Disease 1, 10–19. https://doi.org/10.1007/s42764-019-00002-w

Han, P., Chang, C.-P., 2015. Long non-coding RNA and chromatin remodeling. RNA Biology 12, 1094–1098. https://doi.org/10.1080/15476286.2015.1063770

Hanahan, D., Weinberg, R.A., 2011. Hallmarks of cancer: The next generation. Cell. https://doi.org/10.1016/j.cell.2011.02.013

Hock, E.M., Maniecka, Z., Hruska-Plochan, M., Reber, S., Laferrière, F., Sahadevan M.K., S., Ederle, H., Gittings, L., Pelkmans, L., Dupuis, L., Lashley, T., Ruepp, M.D., Dormann, D., Polymenidou, M., 2018. Hypertonic Stress Causes Cytoplasmic Translocation of Neuronal, but Not Astrocytic, FUS due to Impaired Transportin Function. Cell Reports 24, 987-1000.e7. https://doi.org/10.1016/J.CELREP.2018.06.094

HT-29: Human Colorectal Adenocarcinoma Cell Line (ATCC HTB-38) | Memorial Sloan Kettering Cancer Center [WWW Document], n.d. URL https://www.mskcc.org/research-advantage/support/technology/tangible-material/human-colorectal-adenocarcinoma-cell-line-ht-29 (accessed 7.18.22).

Huarte, M., 2015. The emerging role of lncRNAs in cancer. Nature Medicine 21, 1253–1261. https://doi.org/10.1038/nm.3981

Iarovaia, O. v., Rubtsov, M., Ioudinkova, E., Tsfasman, T., Razin, S. v., Vassetzky, Y.S., 2014. Dynamics of double strand breaks and chromosomal translocations. Molecular Cancer 13, 1–10. https://doi.org/10.1186/1476-4598-13-249/FIGURES/2

Imbriano, C., Gnesutta, N., Mantovani, R., 2012. The NF-Y/p53 liaison: Well beyond repression. Biochimica et Biophysica Acta (BBA) - Reviews on Cancer 1825, 131–139. https://doi.org/10.1016/J.BBCAN.2011.11.001

Izumi, Y., Yang, W., Zhu, J., Burg, M.B., Ferraris, J.D., 2015. RNA-Seq analysis of high NaCl-induced gene expression. Physiological Genomics 47, 500–513. https://doi.org/10.1152/physiolgenomics.00057.2015.-High

Jackson, S.P., Bartek, J., 2009. The DNA-damage response in human biology and disease. Nature 461, 1071–1078. https://doi.org/10.1038/nature08467

Jalali, S., Kapoor, S., Sivadas, A., Bhartiya, D., Scaria, V., 2015. Computational approaches towards understanding human long non-coding RNA biology. Bioinformatics 31, 2241–2251. https://doi.org/10.1093/bioinformatics/btv148

Jeggo, P.A., Löbrich, M., 2007. DNA double-strand breaks: their cellular and clinical impact? Oncogene 26, 7717–7719. https://doi.org/10.1038/SJ.ONC.1210868

Johnson, R.D., Jasin, M., 2000. Sister chromatid gene conversion is a prominent double-strand break repair pathway in mammalian cells. The EMBO Journal 19, 3398–407. https://doi.org/10.1093/emboj/19.13.3398

Kavanagh, J.N., Redmond, K.M., Schettino, G., Prise, K.M., 2013. DNA Double Strand Break Repair: A Radiation Perspective. Antioxidants & Redox Signaling 18, 2458–2472. https://doi.org/10.1089/ars.2012.5151

Kong, Y., Hsieh, C.H., Alonso, L.C., 2018. ANRIL: A lncRNA at the CDKN2A/B locus with roles in cancer and metabolic disease. Frontiers in Endocrinology 9, 405. https://doi.org/10.3389/FENDO.2018.00405/BIBTEX

Krajewska, M., Fehrmann, R.S.N., de Vries, E.G.E., van Vugt, M.A.T.M., 2015. Regulators of homologous recombination repair as novel targets for cancer treatment. Frontiers in Genetics 6, 96. https://doi.org/10.3389/FGENE.2015.00096/BIBTEX

Kumar, R., DuMond, J.F., Khan, S.H., Brad Thompson, E., He, Y., Burg, M.B., Ferraris, J.D., 2020. NFAT5, which Protects against Hypertonicity, is Activated by that Stress via Structuring of its Intrinsically Disordered domain. Proceedings of the National Academy of Sciences of the United States of America 117, 20292–20297. https://doi.org/10.1073/PNAS.1911680117/SUPPL_FILE/PNAS.1911680117.SAPP.PDF

Kumari, R., Jat, P., 2021. Mechanisms of Cellular Senescence: Cell Cycle Arrest and Senescence Associated Secretory Phenotype. Frontiers in Cell and Developmental Biology 9, 485. https://doi.org/10.3389/FCELL.2021.645593/BIBTEX

Lamarche, B.J., Orazio, N.I., Weitzman, M.D., 2010. The MRN complex in double-strand break repair and telomere maintenance. FEBS Letters 584, 3682–3695. https://doi.org/10.1016/J.FEBSLET.2010.07.029

Latgé, G., Poulet, C., Bours, V., Josse, C., Jerusalem, G., 2018. Natural Antisense Transcripts: Molecular Mechanisms and Implications in Breast Cancers. International Journal of Molecular Sciences 19. https://doi.org/10.3390/IJMS19010123

Lee, N., Kim, D., Kim, W.U., 2019. Role of NFAT5 in the immune sustem and pathogenisis of autoimmune disease. Frontiers in Immunology 10, 270. https://doi.org/10.3389/FIMMU.2019.00270/BIBTEX

Leslie, T.K., James, A.D., Zaccagna, F., Grist, J.T., Deen, S., Kennerley, A., Riemer, F., Kaggie, J.D., Gallagher, F.A., Gilbert, F.J., Brackenbury, W.J., 2019. Sodium homeostasis in the tumour microenvironment. Biochim Biophys Acta Rev Cancer 1872, 188304. https://doi.org/10.1016/J.BBCAN.2019.07.001

Lettieri-Barbato, D., Aquilano, K., Punziano, C., Minopoli, G., Faraonio, R., 2022. MicroRNAs, Long Non-Coding RNAs, and Circular RNAs in the Redox Control of Cell Senescence. Antioxidants 11, 480. https://doi.org/10.3390/antiox11030480

Li, J., Sun, H., Huang, Y., Wang, Y., Liu, Y., Chen, X., 2019. Pathways and assays for DNA double-strand break repair by homologous recombination. Acta Biochimica et Biophysica Sinica 51, 879–889. https://doi.org/10.1093/abbs/gmz076

Li, Y., Luo, K., Yin, Y., Wu, C., Deng, M., Li, L., Chen, Y., Nowsheen, S., Lou, Z., Yuan, J., 2017. USP13 regulates the RAP80-BRCA1 complex dependent DNA damage response. Nature Communications 2017 8:1 8, 1–12. https://doi.org/10.1038/ncomms15752

Lieber, M.R., 2010. The Mechanism of Double-Strand DNA Break Repair by the Nonhomologous DNA End-Joining Pathway. Annual Review of Biochemistry 79, 181–211. https://doi.org/10.1146/annurev.biochem.052308.093131

Ling, H., Vincent, K., Pichler, M., Fodde, R., Berindan-Neagoe, I., Slack, F.J., Calin, G.A., 2015. Junk DNA and the long non-coding RNA twist in cancer genetics. Oncogene 34, 5003–5011. https://doi.org/10.1038/onc.2014.456

Long, Y., Wang, X., Youmans, D.T., Cech, T.R., 2017. How do lncRNAs regulate transcription? Science Advances 3, eaao2110. https://doi.org/10.1126/sciadv.aao2110

Ma, C.J., Gibb, B., Kwon, Y., Sung, P., Greene, E.C., 2017. Protein dynamics of human RPA and RAD51 on ssDNA during assembly and disassembly of the RAD51 filament. Nucleic Acids Research 45, 749–761. https://doi.org/10.1093/NAR/GKW1125

Macůrek, L., Lindqvist, A., Voets, O., Kool, J., Vos, H.R., Medema, R.H., 2010. Wip1 phosphatase is associated with chromatin and dephosphorylates γH2AX to promote checkpoint inhibition. Oncogene 29, 2281–2291. https://doi.org/10.1038/onc.2009.501

Manickavinayaham, S., Velez-Cruz, R., Biswas, A.K., Chen, J., Guo, R., Johnson, D.G., 2020. The E2F1 transcription factor and RB tumor suppressor moonlight as DNA repair factors. Cell Cycle 19, 2260–2269. https://doi.org/10.1080/15384101.2020.1801190

Mao, Z., Bozzella, M., Seluanov, A., Gorbunova, V., 2008. Comparison of nonhomologous end joining and homologous recombination in human cells. DNA Repair (Amst) 7, 1765–71. https://doi.org/10.1016/j.dnarep.2008.06.018

Merighi, A., Gionchiglia, N., Granato, A., Lossi, L., 2021. The Phosphorylated Form of the Histone H2AX (γH2AX) in the Brain from Embryonic Life to Old Age. Molecules 26, 7198. https://doi.org/10.3390/molecules26237198

Meseure, D., Vacher, S., Alsibai, K.D., Nicolas, A., Chemlali, W., Caly, M., Lidereau, R., Pasmant, E., Callens, C., Bieche, I., 2016. Expression of ANRIL-polycomb complexes-CDKN2A/B/ARF genes in breast tumors: Identification of a two-gene (EZH2/CBX7) signature with independent prognostic value. Molecular Cancer Research 14, 623–633.

https://doi.org/10.1158/1541-7786.MCR-15-0418/80570/AM/EXPRESSION-OF-ANRIL-POLYCOMB-COMPLEXES-CDKN2A-B

Miermont, A., Lee, S.W.L., Adriani, G., Kamm, R.D., 2019. Quantitative screening of the effects of hyper-osmotic stress on cancer cells cultured in 2- or 3-dimensional settings. Scientific Reports 2019 9:1 9, 1–10. https://doi.org/10.1038/s41598-019-50198-w

Moon, S.-H., Nguyen, T.-A., Darlington, Y., Lu, X., Donehower, L.A., 2010. Dephosphorylation of γ-H2AX by WIP1: An important homeostatic regulatory event in DNA repair and cell cycle control. Cell Cycle 9, 2092–2096. https://doi.org/10.4161/cc.9.11.11810

Nikolova, T., Dvorak, M., Jung, F., Adam, I., Krämer, E., Gerhold-Ay, A., Kaina, B., 2014. The γH2AX Assay for Genotoxic and Nongenotoxic Agents: Comparison of H2AX Phosphorylation with Cell Death Response. Toxicological Sciences 140, 103–117. https://doi.org/10.1093/TOXSCI/KFU066

Peng, C., Hu, W., Weng, X., Tong, R., Cheng, S., Ding, C., Xiao, H., Lv, Z., Xie, H., Zhou, L., Wu, J., Zheng, S., 2017. Over Expression of Long Non-Coding RNA PANDA Promotes Hepatocellular Carcinoma by Inhibiting Senescence Associated Inflammatory Factor IL8. Scientific Reports 7, 4186. https://doi.org/10.1038/s41598-017-04045-5

Pikor, L., Thu, K., Vucic, E., Lam, W., 2013. The detection and implication of genome instability in cancer. Cancer and Metastasis Reviews 32, 341–352. https://doi.org/10.1007/s10555-013-9429-5

Podhorecka, M., Skladanowski, A., Bozko, P., 2010. H2AX Phosphorylation: Its Role in DNA Damage Response and Cancer Therapy. Journal of Nucleic Acids. https://doi.org/10.4061/2010/920161

Polo, S.E., Blackford, A.N., Chapman, J.R., Baskcomb, L., Gravel, S., Rusch, A., Thomas, A., Blundred, R., Smith, P., Kzhyshkowska, J., Dobner, T., Taylor, A.M.R., Turnell, A.S., Stewart, G.S., Grand, R.J., Jackson, S.P., 2012. Regulation of DNA-end resection by hnRNPU-like proteins promotes DNA double-strand break signaling and repair. Molecular Cell 45, 505. https://doi.org/10.1016/J.MOLCEL.2011.12.035

Popov, N., Gil, J., 2010. Epigenetic regulation of the INK4b-ARF-INK4a locus: In sickness and in health. Epigenetics 5, 685. https://doi.org/10.4161/EPI.5.8.12996

Prensner, J.R., Chinnaiyan, A.M., 2011. The emergence of lncRNAs in cancer biology. Cancer Discovery 1, 391–407. https://doi.org/10.1158/2159-8290.CD-11-0209

Puvvula, P.K., 2019. LncRNAs Regulatory Networks in Cellular Senescence. International Journal of Molecular Sciences 20. https://doi.org/10.3390/ijms20112615

Puvvula, P.K., Desetty, R.D., Pineau, P., Marchio, A., Moon, A., Dejean, A., Bischof, O., 2014. Long noncoding RNA PANDA and scaffold-attachment-factor SAFA control senescence entry and exit. Nature Communications 2014 5:1 5, 1–16. https://doi.org/10.1038/ncomms6323

Qiu, S., Huang, J., 2021. MRN complex is an essential effector of DNA damage repair. Journal of Zhejiang University Science B 22, 31–37. https://doi.org/10.1631/jzus.B2000289

Ricoul, M., Gnana Sekaran, T.S., Brochard, P., Herate, C., Sabatier, L., 2019. γ-H2AX Foci Persistence at Chromosome Break Suggests Slow and Faithful Repair Phases Restoring Chromosome Integrity. Cancers (Basel) 11, 1397. https://doi.org/10.3390/cancers11091397

Ruiz-Villalba, A., van Pelt-Verkuil, E., Gunst, Q.D., Ruijter, J.M., van den Hoff, M.J., 2017. Amplification of nonspecific products in quantitative polymerase chain reactions (qPCR). Biomolecular Detection and Quantification 14, 7. https://doi.org/10.1016/J.BDQ.2017.10.001

Russell, W.C., Graham, F.L., Smiley, J., Nairn, R., 1977. Characteristics of a Human Cell Line Transformed by DNA from Human Adenovirus Type 5. Journal of General Virology 36, 59–72. https://doi.org/10.1099/0022-1317-36-1-59

Salguero, I., Belotserkovskaya, R., Coates, J., Sczaniecka-Clift, M., Demir, M., Jhujh, S., Wilson, M.D., Jackson, S.P., 2019. MDC1 PST-repeat region promotes histone H2AX-independent chromatin association and DNA damage tolerance. Nature Communications 10, 5191. https://doi.org/10.1038/s41467-019-12929-5

Schmitt, A.M., Chang, H.Y., 2016. Long Noncoding RNAs in Cancer Pathways. Cancer Cell 29, 452–463. https://doi.org/10.1016/j.ccell.2016.03.010

Sfeir, A., Symington, L.S., 2015. Microhomology-Mediated End Joining: A Back-up Survival Mechanism or Dedicated Pathway? Trends in Biochemical Sciences 40, 701–714. https://doi.org/10.1016/j.tibs.2015.08.006

Sharma, V., Khurana, S., Kubben, N., Abdelmohsen, K., Oberdoerffer, P., Gorospe, M., Misteli, T., 2015. A BRCA1-interacting lncRNA regulates homologous recombination. EMBO Reports 16, 1520–1534. https://doi.org/10.15252/embr.201540437

Sharma, V., Misteli, T., 2013. Noncoding RNAs in DNA damage and Repair. FEBS Letters 587, 1832. https://doi.org/10.1016/J.FEBSLET.2013.05.006

Shen, Z., 2011. Genomic instability and cancer: an introduction. Journal of Molecular Cell Biology 3, 1–3. https://doi.org/10.1093/JMCB/MJQ057

Shi, W., Wang, Q., Bian, Y., Fan, Y., Zhou, Y., Feng, T., Li, Z., Cao, X., 2019. Long noncoding RNA PANDA promotes esophageal squamous carcinoma cell progress by dissociating from NF-YA but interact with SAFA. Pathology - Research and Practice 215, 152604. https://doi.org/10.1016/j.prp.2019.152604

Shopland, L.S., Lynch, C.R., Peterson, K.A., Thornton, K., Kepper, N., von Hase, J., Stein, S., Vincent, S., Molloy, K.R., Kreth, G., Cremer, C., Bult, C.J., O'Brien, T.P., 2006. Folding and organization of a contiguous chromosome region according to the gene distribution pattern in primary genomic sequence. Journal of Cell Biology 174, 27–38. https://doi.org/10.1083/JCB.200603083

Shrivastav, M., de Haro, L.P., Nickoloff, J.A., 2008. Regulation of DNA double-strand break repair pathway choice. Cell Research | 18, 134–147. https://doi.org/10.1038/cr.2007.111

Soniat, M.M., Myler, L.R., Kuo, H.C., Paull, T.T., Finkelstein, I.J., 2019. RPA Phosphorylation Inhibits DNA Resection. Molecular Cell 75, 145-153.e5. https://doi.org/10.1016/J.MOLCEL.2019.05.005

Stöhr, D., Rehm, M., 2021. Linking hyperosmotic stress and apoptotic sensitivity. The FEBS Journal 288, 1800–1803. https://doi.org/10.1111/FEBS.15520

Stucki, M., Jackson, S.P., 2006. γH2AX and MDC1: Anchoring the DNA-damage-response machinery to broken chromosomes. DNA Repair 5, 534–543. https://doi.org/10.1016/J.DNAREP.2006.01.012

Su, M., Wang, H., Wang, W., Wang, Y., Ouyang, L., Pan, C., Xia, L., Cao, D., Liao, Q., 2018. LncRNAs in DNA damage response and repair in cancer cells. Acta Biochimica et Biophysica Sinica 50, 433–439. https://doi.org/10.1093/abbs/gmy022

Subramanian, M., Jones, M.F., Lal, A., 2013. Long Non-Coding RNAs Embedded in the Rb and p53 Pathways. Cancers 2013, Vol. 5, Pages 1655-1675 5, 1655–1675. https://doi.org/10.3390/CANCERS5041655

Sun, F., Liang, W., Qian, J., 2019. The identification of CRNDE, H19, UCA1 and HOTAIR as the key lncRNAs involved in oxaliplatin or irinotecan resistance in the chemotherapy of colorectal cancer based on integrative bioinformatics analysis. Molecular Medicine Reports 20, 3583–3596. https://doi.org/10.3892/MMR.2019.10588/HTML

Swift, M.L., Beishline, K., Flashner, S., Azizkhan-Clifford, J., 2021. DSB repair pathway choice is regulated by recruitment of 53BP1 through cell cycle-dependent regulation of Sp1. Cell Reports 34. https://doi.org/10.1016/J.CELREP.2021.108840

Syed, A., Tainer, J.A., 2018. The MRE11-RAD50-NBS1 Complex Conducts the Orchestration of Damage Signaling and Outcomes to Stress in DNA Replication and Repair. Annual Review of Biochemistry 87, 263–294. https://doi.org/10.1146/annurev-biochem

Tehrani, S.S., Karimian, A., Parsian, H., Majidinia, M., Yousefi, B., 2018. Multiple Functions of Long Non-Coding RNAs in Oxidative Stress, DNA Damage Response and Cancer Progression. Journal of Cellular Biochemistry 119, 223–236. https://doi.org/10.1002/jcb.26217

Thapar, R., 2018. Regulation of DNA Double-Strand Break Repair by Non-Coding RNAs. Molecules 23, 2789. https://doi.org/10.3390/molecules23112789

Torgovnick, A., Schumacher, B., 2015. DNA repair mechanisms in cancer development and therapy. Frontiers in Genetics 6. https://doi.org/10.3389/FGENE.2015.00157

Touceda-Suárez, M., Kita, E.M., Acemel, R.D., Firbas, P.N., Magri, M.S., Naranjo, S., Tena, J.J., Gómez-Skarmeta, J.L., Maeso, I., Irimia, M., 2020. Ancient Genomic Regulatory Blocks Are a Source for Regulatory Gene Deserts in Vertebrates after Whole-Genome Duplications. Molecular Biology and Evolution 37, 2857–2864. https://doi.org/10.1093/MOLBEV/MSAA123

Wan, G., Mathur, R., Hu, X., Liu, Y., Zhang, X., Peng, G., Lu, X., 2013. Long non-coding RNA ANRIL (CDKN2B-AS) is induced by the ATM-E2F1 signaling pathway. Cell Signal 25, 1086–95. https://doi.org/10.1016/j.cellsig.2013.02.006

Wang, J., Aroumougame, A., Lobrich, M., Li, Y., Chen, D., Chenj, J., Gong, Z., 2014. PTIP associates with Artemis to dictate DNA repair pathway choice. Genes & Development 28, 2693–2698. https://doi.org/10.1101/GAD.252478.114

Williams, R.S., Williams, J.S., Tainer, J.A., 2007. Mre11–Rad50–Nbs1 is a keystone complex connecting DNA repair machinery, double-strand break signaling, and the chromatin template. Biochemistry and Cell Biology 85, 509–520. https://doi.org/10.1139/O07-069

Yao, Y., Dai, W., 2014. Genomic Instability and Cancer. Journal of Carcinogenesis & Mutagenesis 5. https://doi.org/10.4172/2157-2518.1000165

Yarmishyn, A.A., Kurochkin, I. v., 2015. Long non-coding RNAs: A potential novel class of cancer biomarkers. Frontiers in Genetics 6, 145. https://doi.org/10.3389/FGENE.2015.00145/BIBTEX

Zhang, Linlin, Liu, F., Wu, L., Fu, S., Xing, L., Zhang, Lianghui, Wang, X., Wang, Y., 2021. Disorder of three-dimensional chromosome structure plays a role in carcinogenesis. Clinical and Translational Discovery 1. https://doi.org/10.1002/ctd2.17

Zhang, R., Xia, L.Q., Lu, W.W., Zhang, J., Zhu, J.S., 2016. LncRNAs and cancer. Oncology Letters 12, 1233–1239. https://doi.org/10.3892/ol.2016.4770

Zhao, F., Kim, W., Kloeber, J.A., Lou, Z., 2020. DNA end resection and its role in DNA replication and DSB repair choice in mammalian cells. Experimental & Molecular Medicine 2020 52:10 52, 1705–1714. https://doi.org/10.1038/s12276-020-00519-1

Zhou, J., Zhou, X.A., Zhang, N., Wang, J., 2020. Evolving insights: how DNA repair pathways impact cancer evolution. Cancer Biology & Medicine 17, 805. https://doi.org/10.20892/J.ISSN.2095-3941.2020.0177